EDO CORPORATION

COLLEGE POINT, NEW YORK, U. S

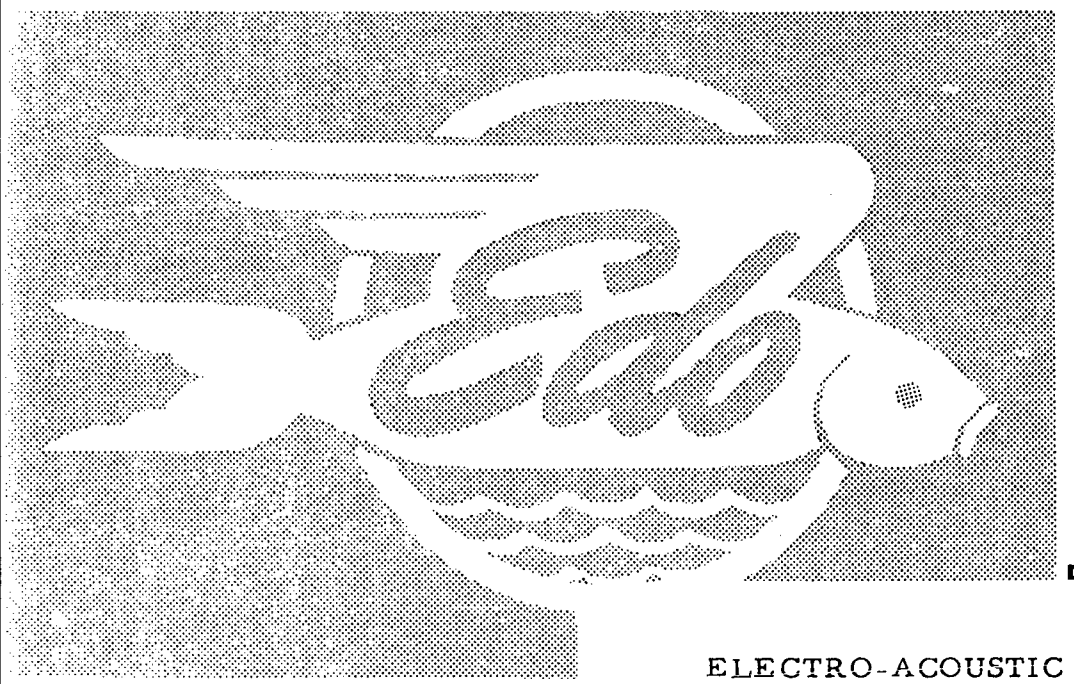

ELECTRO-ACOUSTIC PROPERTIES

of

THE UNDERWATER SPARK DISCHARGE

Contract No. NOnr 2288(00)

Written by:
Sheldon Gardner

Approved by:
C. J. Loda

EDO CORPORATION
COLLEGE POINT, NEW YORK, U.S.A

ABSTRACT

The underwater spark discharge is a means of converting electrical to acoustic energy. In this process, the medium is a fundamental part of the transduction process. An underwater spark discharge is formed by switching an energy storage capacitor at a high voltage to a pair of submerged electrodes. An ionized plasma at high temperature and pressure is formed between the electrodes. The pressure within the plasma is transmitted to the surrounding water as a wave of compression similar to the shock wave created by an underwater explosion.

An analysis of the electro-acoustic properties of the underwater spark is presented. The analysis is based upon expressing the macroscopic properties of the gaseous plasma in terms of equations for the conservation of mass and momentum. The non-compressive approximation is used together with the assumption of adiabatic expansion, to derive and solve an equation of motion for the plasma radius as a function of time. From the radius-time relationship, formulas for the plasma pressures and spark channel wall velocity are derived.

The sonic energy radiated from the underwater spark discharge is discussed, and the directional properties of the radiated pressure are derived.

Properties of the underwater spark discharge plasma as a circuit element are investigated. An electrical equivalent for the discharge circuit is developed from a knowledge of the variation of channel area with time. The time varying plasma resistance is used in the differential

equation of the circuit, and solutions are obtained for the current and voltage waveforms.

The theoretical results are compared with experimental for a fresh water underwater spark discharge having the following parameters, electrode voltage, v = 30 kilovolts, storage capacity, C = . 1 microfarads, and gap separation, L = 4 cm. Considering the nature of the approximations made in the development of the theory, good agreement with experimental results are obtained. In particular, the theoretical dependence of the spark channel radius upon time is found to agree with the experimental results of several investigators.

The theory developed has resulted in an improved understanding of the processes encountered in an underwater spark discharge. Quantities which are extremely difficult to measure in the laboratory may now be predicted. For example, it is found that for the spark discharge parameters stated above, the spark channel formed has an initial radius of about . 4 millimeters and an internal pressure of 12, 000 atmospheres.

TABLE OF CONTENTS

TABLE OF FIGURES

I. INTRODUCTION

An underwater spark discharge is produced when the energy from a high potential source is rapidly transferred to a set of submerged electrodes. Upon the breakdown of the water gap, a plasma of ionized gas forms between the electrodes resulting in a rapid discharge of the energy source. Since the inertia of the surrounding water exerts an almost rigid opposition to the expansion of the spark channel formed, extremely high pressures are developed. Investigators have reported channel pressures in excess of 10,000 atmospheres and temperatures greater than 40,000°K.

A schematic diagram of the type of electrical circuit and electrode assembly used to produce an underwater spark discharge is shown in figure 1. When the switch tube is fired, the high voltage is transferred to the electrodes. The high intensity electric field developed across the gap causes the ionization of the water molecules and the formation of the gaseous plasma.

Edward A. Martin[1] reports upon an extensive investigation into the properties of the discharge plasma. A Kerr Cell photograph made by Martin of a 25 kilovolt spark discharge plasma at 4.1 microseconds is shown in figure 2.

Through electrical measurements made upon the discharge circuit and Kerr Cell photographs of the plasma, Martin was able to calculate the energy distribution among the circuit components and plasma at different times during the discharge. The plasma energy calculations were then compared to the energy which the constituent particles of the spark

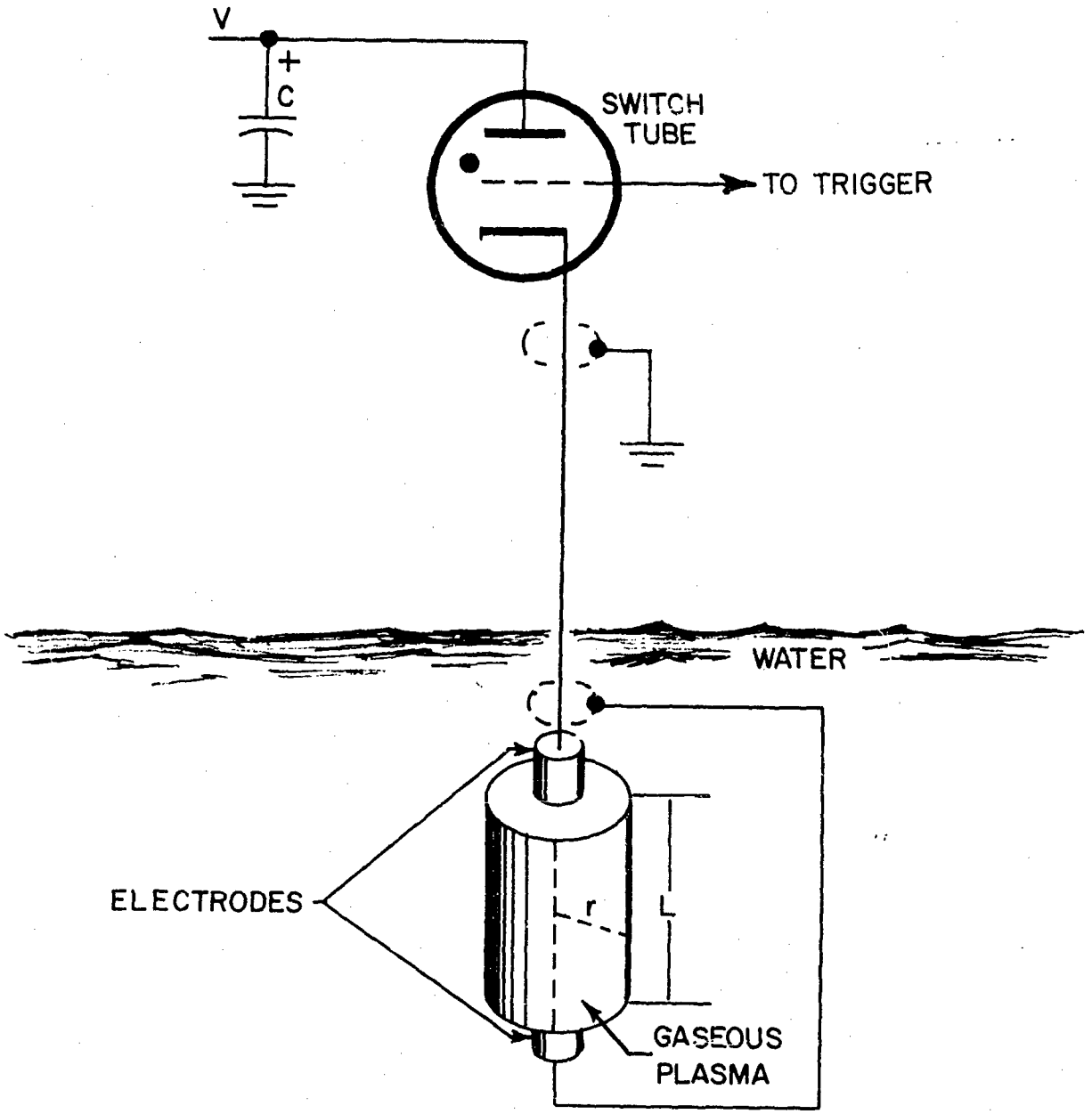

Figure 1. Underwater Spark Discharge Circuit

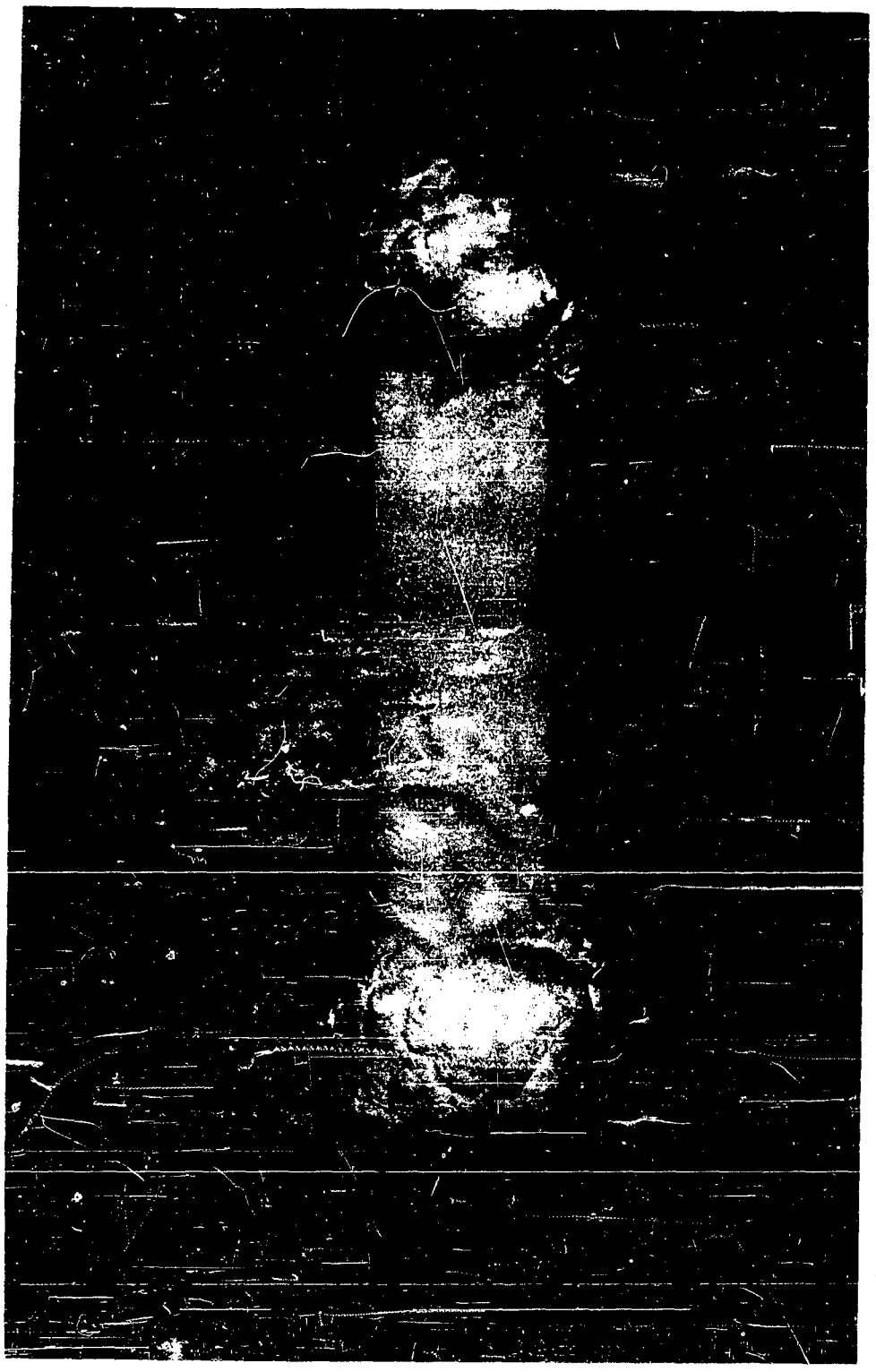

Figure 2. Twenty-Five-Kilovolt Spark at 4.1 Microseconds

channel would store at the experimentally determined temperature and pressure.

The electro-acoustic efficiency of the underwater spark discharge has been investigated by two Soviet scientists, N. A. Frolov and D. P. Roi[2]. Their results have indicated that electro-acoustic efficiencies of up to 32 percent can be achieved with spark gap lengths of 5 cm at voltages of 30 kilovolts.

In many respects, the underwater spark discharge possesses the same hydrodynamic and acoustic properties as a small scale underwater explosion[3, 4]. In an underwater explosion, a gas globe consisting of the detonation products is formed at high temperatures and pressures. The inertia of the water and the elastic properties of the gas and water together provide the necessary conditions for an oscillating system and the gas globe undergoes repeated cycles of expansion and contraction. The analogy between the gas globe formed by an underwater explosion, and the underwater spark discharge plasma has been discussed in a published work by the author[5], and will be further demonstrated in this dissertation.

II. FORMATION OF THE GASEOUS PLASMA

Following the application of a high potential to the submerged electrodes, the sequence of events as reported by Martin[1] is as follows;

A formative period of the order of a microsecond exists, during which branched streamers[6] of ionized molecules advance from each electrode until one streamer makes contact with the other electrode. The discharge then takes place through this streamer causing the others to conduct negligible current.

The duration of the formative period may be observed in the current and voltage oscillograms taken from Frolov's and Roi's paper and reproduced in figure 3. For example, with a gap length of 5 cm, approximately 2-1/4 microseconds following the application of 30 kilovolts to the gap, breakdown occurs. The potential across the gap drops abruptly and the rate of rise of current increases. As the gap length is reduced, both the formative time and the time between breakdown and maximum current are reduced. With a reduction in the gap length, the initial drop in the voltage becomes even greater.

At the instant of breakdown, a gaseous plasma at a high pressure and temperature is formed between the electrodes. It is evident that these conditions cannot persist without affecting the surrounding medium. Due to the continuity of pressure through the plasma-water boundary, a high pressure must also exist in the water adjacent to the spark channel. This abrupt increase in pressure when the plasma is formed is propagated

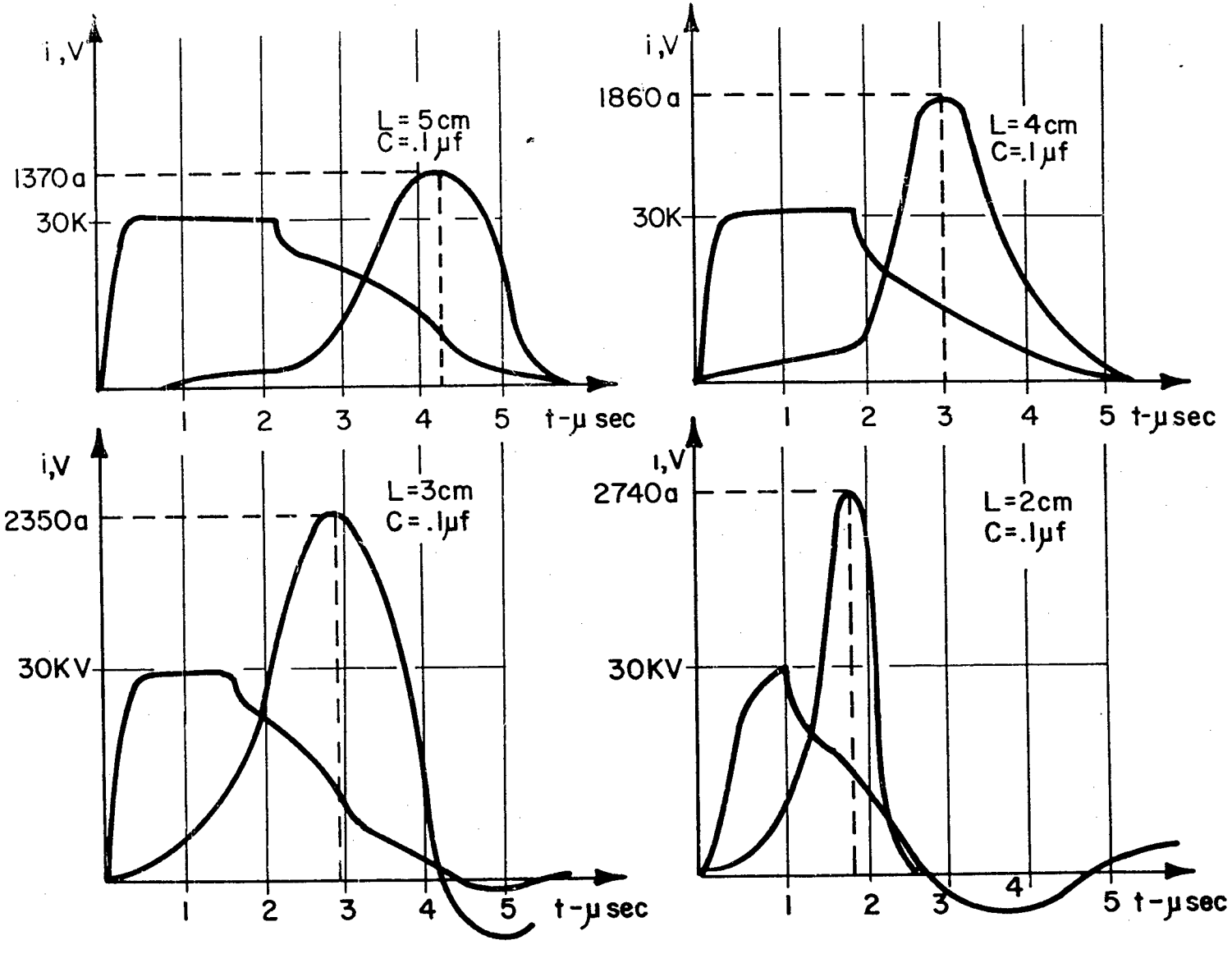

Figure 3 Experimental Underwater Spark Discharge Circuit Waveforms

outward as a wave of compression in the water.

The pressure magnitudes are such that acoustic theory does not apply to the propagation of such a wave. This type of steep-fronted wave whose pressure amplitude is sufficiently great to change the density of the medium is commonly called a "shock" wave[7]. A detailed treatment of the propagation of the cylindrical shock wave generated by the underwater spark discharge is extremely complex and will not be attempted in this dissertation. The interested reader may be referred to several of the references[8, 9].

III. ACOUSTIC PROPERTIES OF THE UNDERWATER SPARK DISCHARGE

1. Basic Relationships

The acoustic properties of the underwater spark discharge may be derived from the equation of motion of the gaseous plasma. Solution of the equation of motion will yield the motion of the plasma boundaries with time. A knowledge of this motion, together with the pressure-volume relationships, enable the pressure within and on the surface of the plasma to be calculated.

An adequate description of the motion of the plasma may be developed if it is assumed that the non-linear nature of the propagation does not affect the energy relationships which govern the differential equations of motion. With this approximation, the energy relationships may be derived on the basis of linear acoustic theory. This technique has been used successfully by several authors in the formulation of the equations of motion for the gas bubble formed by an underwater explosion, where pressures exist which are an order of magnitude greater than the underwater spark discharge[10, 11].

We will use the equations for the conservation of mass and momentum for an ideal fluid medium. These equations may be obtained from any standard text[12, 13] on acoustics or hydrodynamics and are summarized below for convenience.

Conservation of Mass

Let be the density of the fluid, and $\underline{v}$, the vector velocity of a point moving with the fluid; then the equation for the conservation of mass is;

$$(1) \qquad \text{div}\,(\rho\,\underline{v}) = -\frac{\partial \rho}{\partial t}$$

Conservation of Momentum

If p is a scalar pressure distribution which may be a function of time and the spatial coordinates; then Newton's second law requires that,

$$(2) \qquad \text{grad}\, p = -\rho\,\frac{d\underline{v}}{dt}$$

A considerable simplification of these equations results when the non-compressive approximation is made. Physically, this approximation is the assumption that the pressure variations are sufficiently small as to cause a negligible change in the density of the medium. The non-linear effects due to finite compressibility will be discussed further when the propagation of the shock wave due to the underwater spark discharge is discussed in Section 3.12.

Using the non-compressive approximation, remains unchanged with time, and we may modify (1) accordingly,

$$(3) \qquad \text{div}\,\underline{v} = 0$$

In acoustics, just as in electromagnetics, (3) implies the existence of a scalar potential φ whose negative gradient is equal to $\underline{v}$.

$$\underline{v} = -\nabla\varphi \tag{4}$$

The scalar velocity potential φ must be a solution to Laplace's equation which may be obtained by substituting (4) in (3);

$$-\nabla\cdot(\nabla\varphi) = \nabla^2\varphi = 0 \tag{5}$$

Examining (2) we see that if we substitute (4) for $\underline{v}$ we obtain;

$$\nabla p = -\rho \frac{d}{dt}(-\nabla\varphi)$$

or,

$$p = \rho \frac{d\varphi}{dt} \tag{6}$$

Which is the relationship between pressure and velocity potential in an incompressible fluid.

2. Motion of the Gaseous Plasma

Before the equation of motion of the gaseous plasma may be formulated, it is necessary to make several other assumptions:

It is assumed that at the instant of breakdown of the gap, a gaseous plasma having an instantaneous temperature T_o and internal pressure p_o is formed. Furthermore, the shape of the plasma is such that it may be considered a right circular cylinder of length equal to the gap length L, and initial radius, a_o. A uniform energy density throughout the plasma is also assumed.

A diagram of the plasma and the coordinate system which will be employed is shown in figure 4.

In addition, the assumption is made that from the instant of breakdown, some fraction of the original capacitor energy is available for plasma motion. Actually, this energy is supplied at the start of current flow. However, if the plasma motion is slight during the interval, there is little error in treating the energy as available from the beginning of the interval. As a first approximation, the radiation of acoustic energy will be neglected, as well as dissipation of energy by thermal conduction at the plasma-water boundary.

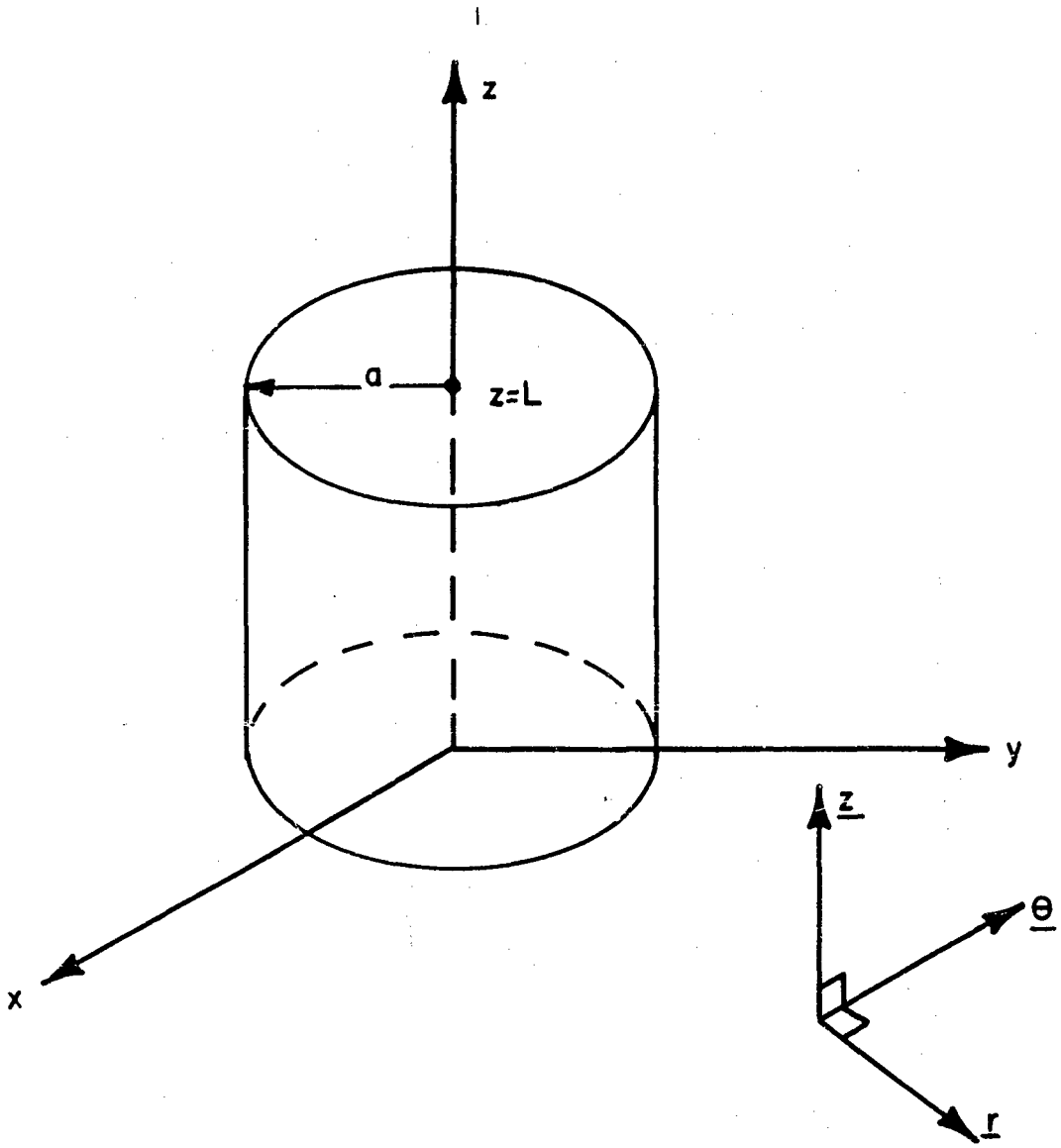

Figure 4 Cylindrical Coordinate System

3. Kinetic Energy of Motion

The kinetic energy of motion is the energy associated with the water by reason of its motion. If spherical instead of cylindrical symmetry existed, this energy could be derived quite simply. We shall then modify the equations to take cylindrical symmetry into account.

Let $u = dr/dt$ be the radial velocity of the fluid at a point r. Then, by virtue of equation (3)

$$\frac{1}{r^2} \frac{\partial}{\partial r} \left\{ r^2 u \right\} = 0 \tag{7}$$

Upon performing the partial differentiation,

$$\frac{1}{r^2} \left\{ 2ru + r^2 \frac{du}{dr} \right\} = 0$$

or,

$$\frac{du}{dr} = - \frac{2u}{r} \tag{8}$$

Applying the boundary condition that at the plasma wall $r = a$, $u_a = da/dt$ and solving for u,

$$u = \frac{a^2}{r^2} \, d\,a/dt \qquad r \geq a \tag{9}$$

Hence, in the water, the particle velocity falls off as the square of the radial distance. Therefore, for the spherical case, the kinetic energy of flow is,

$$\text{K. E.}_S = \int_a^{\infty} \frac{\rho}{2} (4\pi r^2 dr) \left(\frac{a^2}{r^2} \frac{da}{dt} \right)^2$$

$$\text{K. E.}_S = 2\pi\rho a^3 \left(\frac{da}{dt} \right)^2 \tag{10}$$

Now, consider a cylindrical plasma of radius a and length L. In the cylindrical region $a < r < L/2$, the plasma approximates an infinite cylinder, therefore the velocity potential φ falls off approximately as $\frac{1}{r^{\frac{1}{2}}}$. So that by equation (4), the velocity will fall off approximately as $\frac{1}{r^{\frac{3}{2}}}$.

Employing the boundary condition, we find for this region the following approximate expression for the particle velocity;

$$u \approx \left(\frac{a}{r} \right)^{3/2} \frac{da}{dt} \qquad a \leq r \leq L/2 \tag{11}$$

Therefore, the kinetic energy for the region under consideration is,

$$\text{K. E.} \approx \int_a^{L/2} \frac{\rho}{2} \left(\frac{a}{r} \right)^3 \left(\frac{da}{dt} \right)^2 2\pi r L dr$$

$$\text{K. E.} \approx \pi\rho a^3 L \left(\frac{da}{dt} \right)^2 \left[\frac{-1}{r} \right]_a^{L/2}$$

Since the plasma radius is assumed to be much less than L/2, the value of the K. E. at L/2 will be neglected, as well as any contributions for $r > L/2$. Therefore, the kinetic energy of the water is;

$$\text{(11)} \qquad \text{K. E.} \approx \pi \rho a^2 \dot{} \; L \left(\frac{da}{dt} \right)^2$$

4. Potential Energy

The potential energy of the spark channel is the work done by the channel in expanding from a radius a to infinity.

$$(12) \qquad P.E. = \int_a^\infty (p - P)dv = \int_a^\infty (p - \underline{P})\, 2\pi\, aLda$$

P is the hydrostatic pressure at the depth of the discharge, and p is the external plasma pressure. A further physical interpretation of the potential energy as well as the external plasma pressure will be given later in Section 3.7.

5. Equation of Motion

We have assumed that, from the instant of breakdown, the plasma possesses an energy Y which remains constant. On the basis of this assumption, an equation of motion may be written which expresses the conservation of kinetic and potential energy. From (11) and (12);

$$(13) \qquad \pi\rho a^2 L \left(\frac{da}{dt}\right)^2 + \int_a^\infty (p - \underline{P})\, 2\pi a L da = Y$$

Using the fact that at the beginning of the motion when $a = a_o$, $da/dt = 0$;

$$(14) \qquad Y = \int_{a_o}^\infty (p - \underline{P})\, 2\pi a\, L da$$

Y has the physical significance of being the fraction of the initial capacitor energy which is available for plasma motion.

Substituting Equation (14) in Equation (13) we obtain the following equation of motion;

$$(15) \qquad a^2 \left(\frac{da}{dt}\right)^2 = \frac{2}{\rho} \int_{a_o}^a (p - \underline{P})\, a\, da$$

This equation expresses the relationship between the plasma radius, wall velocity, and wall pressure.

Equation (15) may be integrated provided the dependence of p on a is known. If it is assumed that in the expansion of the plasma, no heat is transferred to the surrounding water, an adiabatic law is followed.

6. Adiabatic Expansion

We assume that the underwater spark discharge plasma behaves as an ideal gas. This is not strictly true due to the production of long range interparticle forces by the high degree of ionization. However, we will use the ideal gas law as a first approximation, as Martin does in his calculations. When an ideal gas undergoes a quasistatic adiabatic process;[14]

$$(16) \qquad \begin{cases} dQ = c_v d\theta + pdv = 0 \\ dQ = c_p d\theta - vdp = 0 \end{cases}$$

where, c_v = specific heat at constant volume

c_p = specific heat at constant pressure

$d\theta$ = differential temperature change

Dividing Equations (16)

$$\frac{dp}{p} = -\gamma \frac{dv}{v}$$

or, regarding $\gamma = \frac{c_p}{c_v}$ as constant and integrating;

$$(17) \qquad pv^{\gamma} = p_o v_o^{\gamma} = \text{constant}$$

The ratio of the specific heats γ may be obtained, provided we assume that the plasma formed by the underwater spark discharge behaves as a fully ionized gas. Plasmas of 5 percent ionization are generally considered completely ionized, meaning that the long range interparticle Coulomb forces play a dominant role in determining the plasma properties.

Martin reports that the underwater spark discharge is approximately 30 percent ionized[15]; so that the assumption of "complete" ionization is a reasonable one.

For a fully ionized gas, Spitzer[16] gives the following formula for γ ;

$$\gamma = \frac{2 + m}{m} \tag{18}$$

where the quantity m is the number of external degrees of freedom. Since a heavy current flows, particle motion exists in a direction parallel to the electrodes. In addition, the cylindrical plasma is expanding radially, so that the particles have a radial motion. This argument would seem to imply the existence of two external degrees of freedom resulting in $\gamma = 2$. If the particle velocities were randomized, due to collisions, γ would equal 5/3 which is sufficiently close to $\gamma = 2$ to warrant the use of the value $\gamma = 2$ in subsequent calculations.

The solution obtained by the adiabatic assumption expresses the kinetic* pressure of the plasma as a function of the plasma volume. In the solution of the equation of motion, the external pressure (the pressure which exists in the water adjacent to the spark channel) must be used. The assumption will be made that the kinetic and external pressures are equal. This is not strictly true due to deviations from the ideal gas law. More will be said about the plasma pressures in Section 3.8.

*The pressure used in the ideal gas law, $p_{kinetic}\, v = MRT$

7. Solution of the Equation of Motion

Using the adiabatic approximation for the external pressure, the plasma radius as a function of time will now be obtained. Substitution of the dependence of the external pressure p upon the plasma volume from (17) into (15) results in the following integrodifferential equation for the radius of the underwater spark discharge plasma as a function of time;

$$(19) \qquad a^2 \left(\frac{da}{dt}\right)^2 = \frac{2}{\rho} \int_{a_o}^{a} \left[p_o \left(\frac{a_o}{a}\right)^4 - \underline{P}\right] a\,da$$

We may express the variable a in terms of the non-dimensional variable $x = a/a_o$. The equation becomes;

$$(20) \qquad \left(\frac{da}{dt}\right)^2 = \frac{2}{\rho x^2} \int_{1}^{x} \left(p_o x^{-4} - \underline{P}\right) x\,dx$$

Performing the integration, we obtain;

$$(21) \qquad \frac{da}{dt} = \sqrt{\frac{p_o}{\rho}} \; \frac{\left[1 - x^{-2} + \alpha(1 - x^2)\right]^{1/2}}{x}$$

Where $\alpha = \underline{P}/p_o$, and is generally $<< 1$ during the early stages of the motion.

Separating the variables in (21) and solving for t,

$$(22) \qquad t = a_o \sqrt{\frac{\rho}{p_o}} \int_{1}^{x} \frac{x^2\,dx}{\left[x^2 - 1 + \alpha x^2 (1 - x^2)\right]^{1/2}}$$

Since the early stages of the motion when $\alpha \ll 1$ are of interest, the term involving α may be neglected and the integration of (22)* results in;

$$t = \tau \left\{ x\sqrt{x^2 - 1} + \cosh^{-1} x \right\} \tag{23}$$

where,

$$\tau \equiv \sqrt{\frac{\rho a_o^2}{4p_o}}$$

This is the equation for the variation of the plasma radius with time. An approximation to this expression for $a/a_o > 1.2$ is;

$$t \approx \tau x^2$$

or,

$$a \approx a_o \quad (t/\tau)^{1/2} \tag{25}$$

Equation (23) and the approximation (24) are plotted in figures 5 and 6.

An alternate form of (25) may be derived. Using the adiabatic equation, we may obtain a solution to (14).

The total energy Y is given by;

$$Y = \int_{a_o}^{\infty} (p - \underline{P})\, 2\pi\, a L da \approx \int_{a_o}^{\infty} po \left(\frac{a_o}{a}\right)^4 2\pi\, a L da \tag{26}$$

$$\approx p_o \pi a_o^2 L$$

*Pierce's Table of Integrals P. 22 #150

Substituting (26) into (25), an equivalent expression for the underwater spark discharge plasma radius as a function of time is obtained;

$$(27) \qquad a \approx \left(\frac{4Y}{\pi \rho L} \right)^{1/4} t^{1/2} \qquad a \gg a_o$$

Equation (27) may be derived a bit more directly by a simple physical interpretation of the equation of motion. Let us examine the equation for the potential energy of the plasma obtained from (12);

$$(28) \qquad P.E. = \int_a^\infty p\,dv + \underline{P}\,\pi a^2 L$$

The second term on the right represents the work done by the plasma against hydrostatic pressure. The first term represents the internal energy of the plasma as a function of its radius;

$$(29) \qquad E(a) = \int_a^\infty p\,dv = p_o v_o^2 \int_a^\infty \frac{dv}{v^2} = \frac{p_o v_o^2}{v}$$

This shows that the internal energy decreases as rapidly as a^2; so that for $a >> a_o$, the internal energy becomes negligible compared to the kinetic energy. In the same manner, if $a << a_m$, where a_m is the maximum radius of the plasma, since $p >> \underline{P}$, the hydrostatic term may be neglected in comparison to the kinetic energy. We are then left with an approximate equation of motion,

$$(30) \qquad \pi \rho a^2 L \left(\frac{da}{dt} \right)^2 \approx Y \qquad a_o << a << a_m$$

or

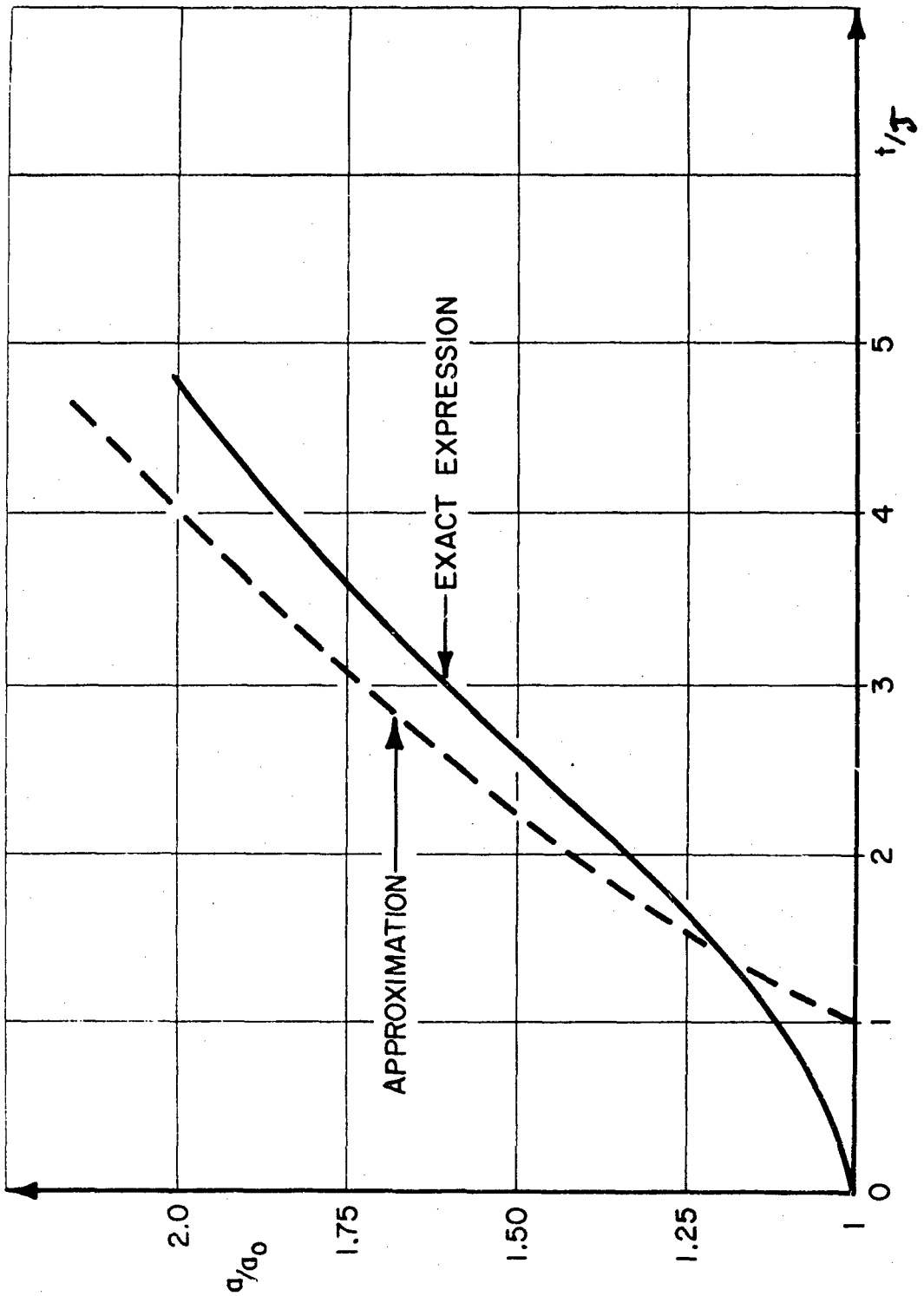

Figure 5 Plasma Radius as a Function of Time

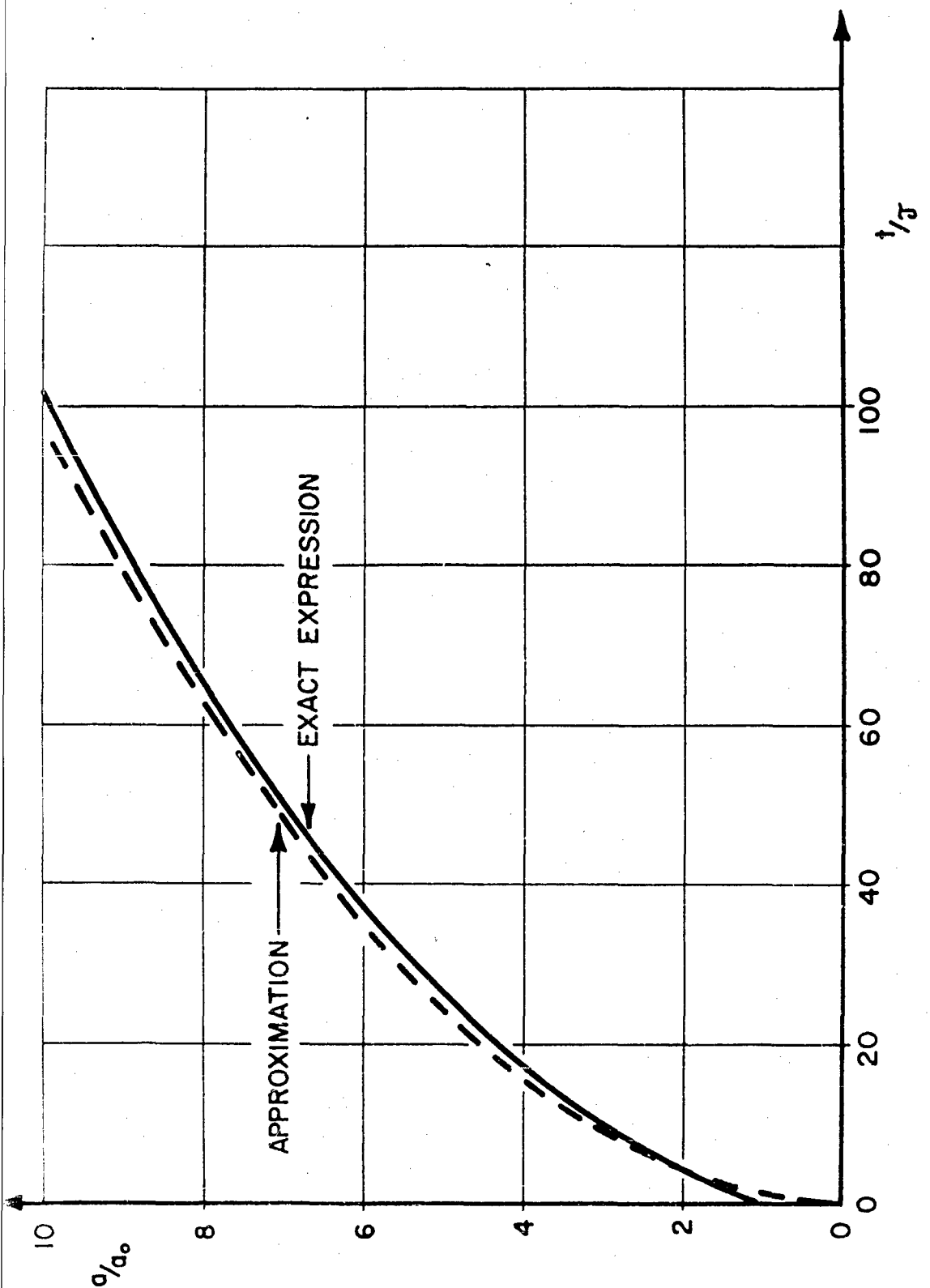

Figure 6 Plasma Radius as a Function of Time

$$(31) \qquad a\left(\frac{da}{dt}\right) \approx \left(\frac{Y}{\pi \rho_o L}\right)^{1/2}$$

Integrating (31);

$$(32) \qquad a \approx \left(\frac{4Y}{\pi \rho L}\right)^{1/4} t^{1/2} \qquad a_o << a << a_m$$

Equation (32) is identical to (27). Both equations show that the spark discharge plasma radius varies as the square root of the time.

Spark Channel Wall Velocity

The wall velocity of the expanding spark channel may be obtained from (21). Neglecting α, the channel wall velocity in the early stages of the motion is,

$$(33) \qquad \frac{da}{dt} = \sqrt{\frac{P_o}{\rho}} \frac{[x^2 - 1]}{x^2}^{1/2} = \frac{a_o}{2\tau} \frac{[x^2 - 1]}{x^2}^{1/2}$$

The maximum wall velocity may be obtained by differentiating (33). It occurs when $a = \sqrt{2}\, a_o$ and;

$$(34) \qquad \frac{da}{dt_{MAX}} = \sqrt{\frac{P_o}{4\rho}} = \frac{a_o}{4\tau}$$

8. Plasma Pressure

In the solution of the equation of motion, we have assumed that the underwater spark discharge plasma obeys the ideal gas law. This law concerns a given amount of a gas at a temperature T. The gas is assumed to have no interparticle forces as well as particles of zero volume. The average pressure which is required to constrain these particles to a given volume is designated as the kinetic pressure of the gas $p_{kinetic}$. The ideal gas law applies to this kinetic pressure and states that;

$$(35) \qquad p_{kinetic}\, v = RT$$

where the gas constant R is related to the universal gas constant R_m in a mixture of j different masses γj by,

$$(36) \qquad R = R_M \sum_j \gamma j / Mj$$

M_j being the molecular weight of the jth component.

The total kinetic pressure is the sum of the partial pressures and;

$$(37) \qquad p_{kinetic} = NKT$$

where,

N = number of particles per unit volume

K = Boltzman's constant = $1.38\ (10)^{-23}$ joules/$^{\circ}$K

If the underwater spark discharge plasma behaved as an ideal gas, the external pressure necessary to constrain the gas, $p_{external}$, would equal $p_{kinetic}$. However, the existence of a high degree of ionization produces long range interparticle forces resulting in additional pressures.

If the particles exert repulsive forces on each other, then the tendency to expand is increased. The increase in the constraining pressure is called $p_{repulsion}$. If there is also an interparticle attraction, the pressure on the constraining envelope is reduced, the reduction being called $p_{attraction}$. It is usual to call the difference of attractive and repulsive pressures $p_{internal}$, which is usually positive.

In addition, if there is a motion of charged particles through the gas, the resultant magnetic field produces average forces tending to force the particles together. This reduces the required envelope pressure by an amount designated as p_{pinch}. More will be said about this pinch pressure when the electrical properties of the discharge are discussed in Section 4.2.

The overall effects of these pressure contributions may be summarized in the following equation,

$$p_{kinetic} = p_{external} + p_{pinch} + p_{internal} \tag{38}$$

Martin[17] has found that the internal pressure has a maximum magnitude of about 1/4 of the external pressure which he obtained by means of the measured wall velocity and shock wave equations.

It is to be noted that in the evaluation of the equation of motion, the external pressure was assumed to be equal to the kinetic pressure. However, the kinetic pressure is greater than the external pressure due to the pinch and internal pressure contributions. This increase will tend to offset the error due to the noncompressive approximation in which lower external pressures than actually exist are assumed.

The kinetic pressure (or external pressure) may be evaluated by means of the adiabatic expansion equation (17);

$$(39) \qquad p_{external} \approx p_{kinetic} = p_o \left(\frac{v_o}{v}\right)^{\gamma} = p_o \left(\frac{a_o}{a}\right)^{4} = p_o/x^4$$

Using (23) for x(t), a plot of p/p_o vs t/τ is shown in figure 7. The similarity of this pressure curve to an exponential decay is evident. In fact, an exponential approximation will be used in the next section. This approximation is shown in figure 7 as a dotted curve and may be written as,

$$(40) \qquad p_{kinetic} \approx p_o \exp- (t/2\tau)$$

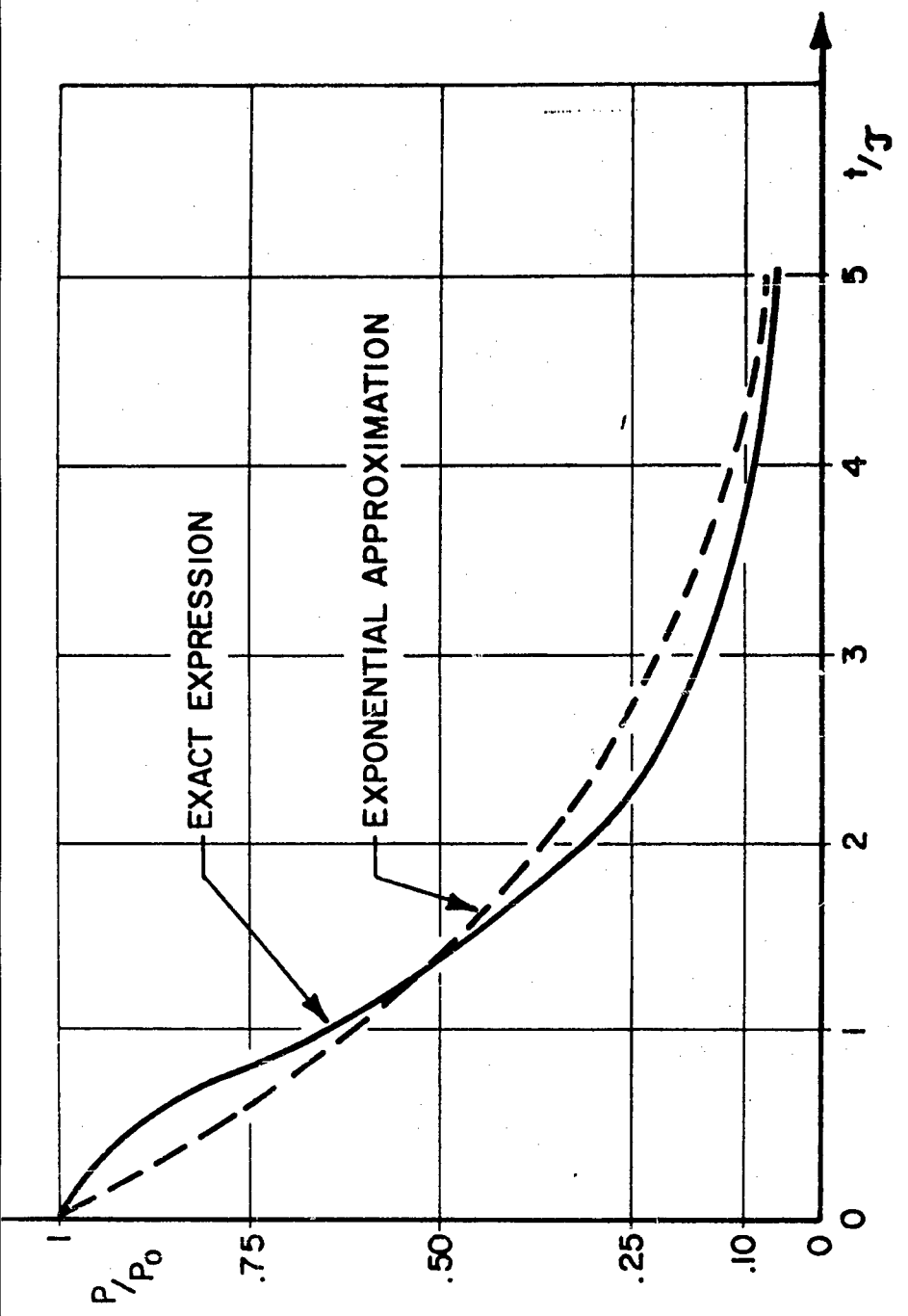

Figure 7 Kinetic Pressure as a Function of Time

9. The Directional Distribution of the Acoustic Radiation

The directional distribution of the acoustic radiation from an underwater spark discharge will now be derived using an acoustic approximation. The plasma column can be considered as a line radiator having a length equal to the gap separation L. For a point R sufficiently far away, lines from different points may be considered parallel. Figure 8 depicts the geometry.

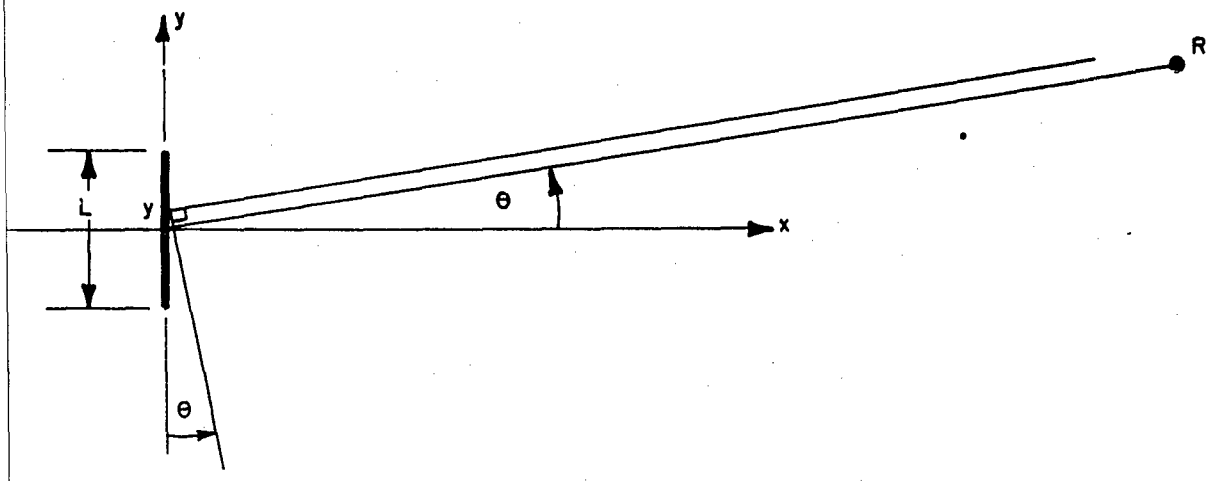

Figure 8. Radiation Geometry

Neglecting travel time from the origin to R, if linearity is assumed, the waveform contribution at R due to an element of length dy, and strength a (y/L), located at y is;

$$dp = f\,(t + y/c \sin\theta)\; a\,(y/L)\; dy \tag{41}$$

Integrating over the length of the column, the waveform at R is;

$$p_R\,(t, \Delta\tau) = \int_{-\infty}^{+\infty} f\,(t + u\Delta\tau)\; a\,(u)\; du \tag{42}$$

where,

$$u = y/L$$

$$\Delta\tau = L/c \sin\theta$$

and

$$\int_{-1/2}^{+1/2} a(u)\, du = 1$$

In the special case, where $f(t) = \delta(t)$, we denote the response by $h_R(t, \Delta\tau)$;

$$(43) \qquad h_R(t, \Delta\tau) = \int_{-\infty}^{+\infty} \delta(t + u\Delta\tau)\, a(u)\, du$$

Using the sifting property of the delta function,

$$(44) \qquad h_R(t, \Delta\tau) = \begin{cases} \dfrac{-a(t/\Delta\tau)}{\Delta\tau} & |t| < |\Delta\tau/2| \\ 0 & |t| > |\Delta\tau/2| \end{cases}$$

Therefore, the conclusion is reached that the plane wave impulse response $h_R(t, \Delta\tau)$ is the same function of $(t/\Delta\tau)$ as the strength distribution is of u.

Using the properties of convolution, the waveform at R due to a line radiator having an amplitude distribution a (u) is,

$$(45) \qquad p_R(t, \Delta\tau) = \int_{-\infty}^{+\infty} \frac{-a(-z/\Delta\tau)}{\Delta\tau} f(t - z)\, dz$$

We will now use equation (44) for an evaluation of the directional distribution of the pressure due to an underwater spark discharge.

If we assume that the strength of the radiated wave is uniform over the length of the discharge plasma;

(46) $$a(u) = U(u + 1/2) - U(u - 1/2)$$

Inserting the above and the exponential approximation $e^{-\alpha t}$ for f(t) into (45), we obtain;

(47) $$p_R(t, \Delta\tau) = \int_{-\Delta\tau/2}^{+\Delta\tau/2} e^{-\alpha(t - z)}\, U(t - z)\, dz$$

where,

α = the reciprocal time constant

Equation (47) is solved in Appendix A. The result is,

(48)

$$p_R(t, \Delta\tau) = \begin{cases} \dfrac{\sinh \alpha\Delta\tau/2}{\alpha\Delta\tau/2}\, e^{-\alpha t} & t \geq \Delta\tau/2 \\ 1/\alpha\Delta\tau \left[1 - e^{-\alpha t_e} - \alpha\Delta\tau/2\right] & -\Delta\tau/2 \leq t \leq \Delta\tau/2 \\ 0 & t \leq -\Delta\tau/2 \end{cases}$$

This solution is plotted in figure 9 as a function of αt for $\alpha L/c = 5$ and $\theta = 0°$, 15°, 30°, 60°, and 90°. At $\theta = 0°$, the waveform is identical to $f(t) = e^{-\alpha t}$, since all contributions arrive simultaneously. At $\theta = 90°$, since $\alpha L/c$ is large compared to the time constant of the waveform, the pressure at R approaches the same form as a (u). f (t) may then be regarded as an impulse.

The peak value of $p_R(t, \Delta\tau)$ occurs at $t = +\Delta\tau/2$ and is,

(49) $$p_{R_{peak}}(\Delta\tau/2, \Delta\tau) = \frac{\left[1 - e^{-\alpha\Delta\tau}\right]}{\alpha\Delta\tau}$$

Equation (49) is plotted in figure 10 as a function of θ with $\alpha L/c$ as a parameter. Since, physically, $\alpha L/c$ represents the ratio of the travel time across the source to the time constant of the waveform, in limit as $\alpha L/c \longrightarrow 0$, the directional dependence vanishes.

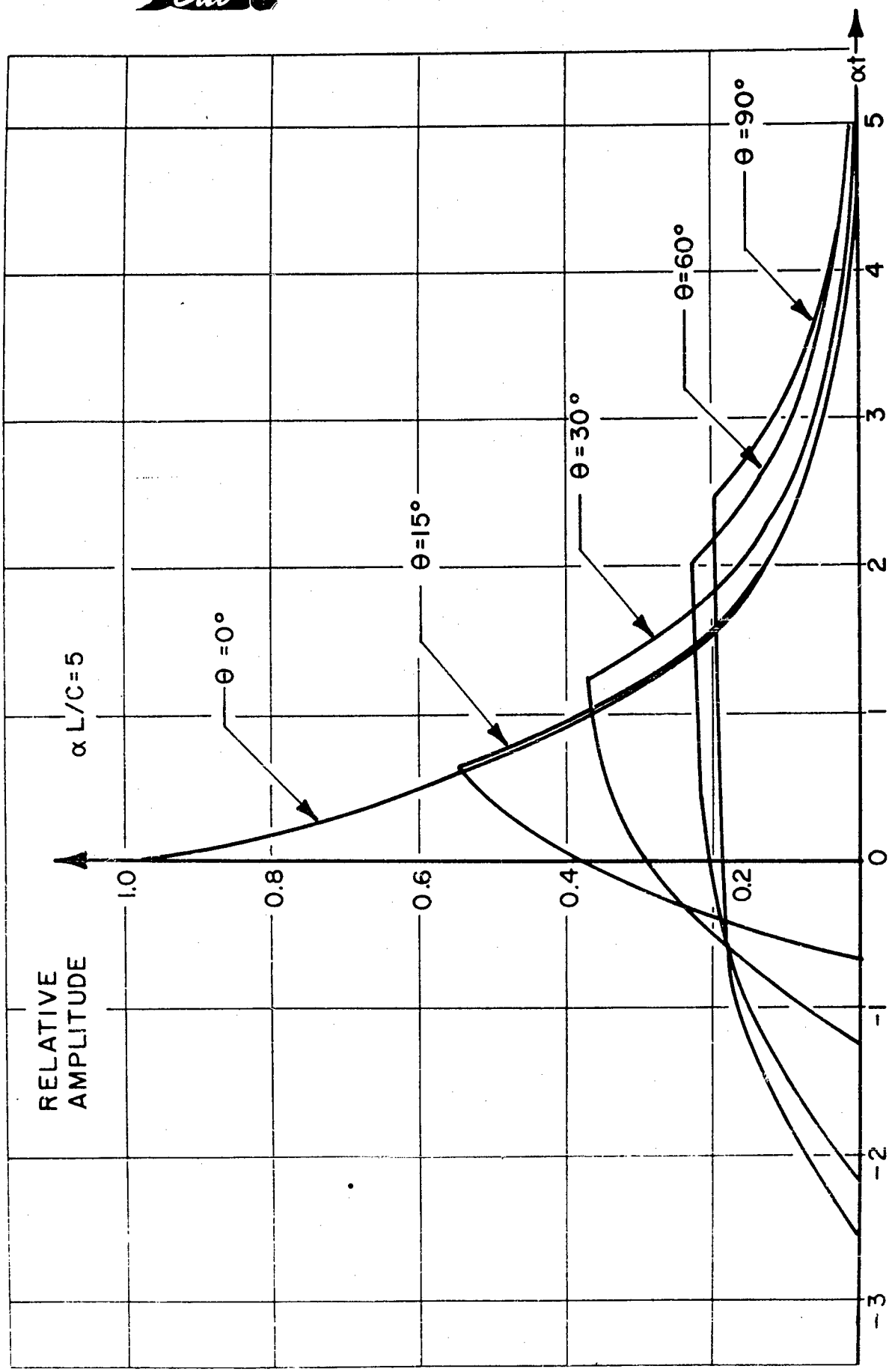

Figure 9 Theoretical Waveforms as a Function of Angle

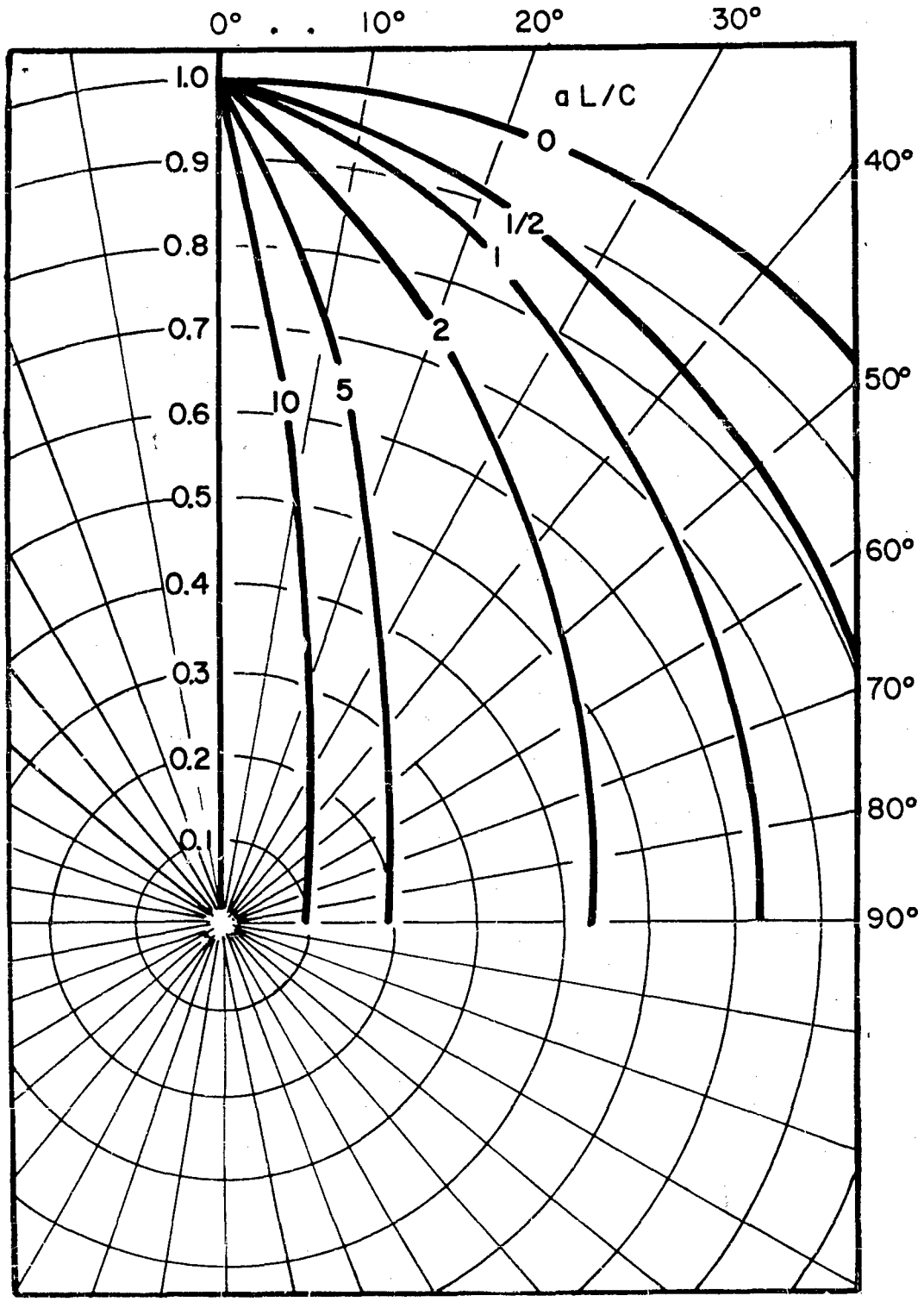

Figure 10 Theoretical Peak Amplitude Patterns

10. Acoustic Energy Flux

The acoustic energy radiated by the underwater spark discharge will be discussed. It was assumed earlier that there was no radiation of acoustic energy. If the solution obtained is taken as a first approximation, it is possible to calculate what energy is actually radiated. First, the energy flux normal to the spark channel will be calculated. If, in addition to this calculation, the directional distribution of radiated energy is obtained, the total energy flux radiated by the underwater spark discharge plasma will be known.

The instantaneous energy flux per unit area per unit time in any direction is,

$$\frac{d\phi}{dt} = \frac{p_r^2}{\rho c} \tag{50}$$

where ρc equals the wave impedance of the medium.

If we consider a direction normal to the spark channel, where $\theta = 0°$, and assume first cylindrical and then spherical spreading, the pressure at a distance r is approximately,

$$p_{r_{normal}} \approx p_{ext.}\left(\frac{a_o}{L/2}\right)^{1/2}\left(\frac{L/2}{r}\right) \approx p_o a_o^4 \left(\frac{a_o}{L/2}\right)^{1/2}\left(\frac{L/2}{r}\right)\frac{1}{a^4} \tag{51}$$

Substituting (51) into (50), and separating variables,

$$d\phi_{normal} = \frac{p_o^2 a_o L}{2 r^2 \rho c} \int_{x=1}^{x=x_1} \frac{dt}{x^8} \tag{52}$$

If dt is substituted from (21)

(53) $$dt = \frac{x^2}{(x^2 - 1)^{1/2}} \; a_o \sqrt{\frac{\rho}{p_o}} \; dx$$

and,

(54) $$\phi_{normal} = \frac{p_o^{3/2} a_o^2 L}{2 r^2 \rho^{1/2} c} \int_{x=1}^{x=x_1} \frac{dx}{x^6 (x^2 - 1)}$$

Since the major part of the integral arises from x near unity, little error will be introduced by letting $x_1 = \infty$. The integral may be easily evaluated* as 4/5 . 2/3 = 8/15.

The expression for ϕ_{normal} becomes,

(55) $$\phi_{normal} = \frac{8}{30} \frac{p_o^{3/2} a_o^2 L}{\rho^{1/2} c r^2}$$

It is interesting to check this result with one obtained by use of the exponential approximation for the external pressure, $p \propto e^{-t/2\tau}$

(56) $$\phi_{normal} = \frac{1}{\rho c} \int_0^{\infty} p_{r_{normal}}^2 \, dt$$

$$\approx \frac{p_o^2 a_o L}{2 r^2 \rho c} \int_0^{\infty} e^{-t/\tau} \, dt \approx \frac{p_o^2 a_o L}{2 r^2 \rho c} \cdot \tau$$

* Successive use of #205 Pierce's Table of Integrals, Ginn & Co. 1929

The normal energy flux becomes,

$$(57)\quad \phi_{\text{normal}} \approx \frac{p_o^{\,2} a_o L}{2r^2 \rho c} \sqrt{\frac{\rho a_o^{\,2}}{4 p_o}} \approx \frac{p_o^{\,3/2} a_o^{\,2} L}{4 \rho^{1/2} c r^2}$$

Therefore, an error of about 3% is introduced by substituting the exponential approximation for the pressure in the calculation of the energy flux normal to the spark channel.

11. Directional Distribution of Radiated Energy

The energy flux radiated in a direction normal to the spark channel has been calculated. The energy flux radiated in directions other than the normal may be calculated by means of the directional distribution of the radiated pressure. An energy flux directivity factor may be defined as the ratio of the integral of the energy flux over a sphere to the normal energy flux;

$$\eta_D \equiv \int_0^{2\pi} \int_0^{\pi} \frac{\phi(\theta, \psi) \sin\theta \, d\theta \, d\psi}{\phi_{\text{normal}}} \tag{58}$$

If $\propto L/c$ is sufficiently small so that $\phi(\theta, \psi) \approx \phi_{\text{normal}}$ then $\eta_D = 1$ and the source is essentially spherical.

In terms of η_D, the total radiated acoustic energy W is,

$$W = 4\pi r^2 \cdot \eta_D \phi_{\text{normal}} = \frac{\pi p_o^{3/2} a_o^2 L}{\rho^{1/2} C} \eta_D \tag{59}$$

The acoustic efficiency η_A may be defined as W/Y. Using (26) for Y;

$$\eta_A \approx \frac{\eta_D}{c} \sqrt{\frac{p_o}{\rho}} \tag{60}$$

The result (61) is significant in that, since in the acoustic approximation there are no energy losses with range, η_A is the fraction of Y actually radiated as acoustic energy. The energy measurable over a sphere of radius R is not W, but slightly less than W, due to energy losses

in shock wave propagation.

The pressure and energy at a point (R, θ) has been evaluated on the basis of the acoustic approximation. Now, the results will be modified to take into account the non-linear nature of the propagation. This procedure, while not being rigorous in the mathematical sense, does give a clear picture of the physical phenomena, as well as numerical results which agree quite well with experimental data.

12. Losses Due to Shock Wave Propagation

A large amount of work, both experimental and theoretical, was done prior to and during World War II in the field of underwater explosions[18, 19, 20]. Several theories were set forth for the propagation of the shock wave formed by the detonation of an underwater explosive[21, 22].

These theories may be applied to the shock wave produced by an underwater spark discharge because of the "principle of similarity." The principle of similarity states that if the linear size of a charge is changed by a factor k, the pressure conditions will remain unchanged if new distance and time scales k times as great as the original ones are used[23]. In the formulation of this principle, all forces not scaling geometrically have been neglected.

For spherical symmetry, the general characteristics of shock wave propagation are such that if the shock pressure is assumed to have the form $pe^{-t/\theta}$ at the charge, the peak pressure will decay at a rate more rapidly than $1/r$ and be only a function of R/a'_o, where a'_o is the initial charge radius.

The time constant θ will increase with R/a'_o representing a broadening of the wave as it propagates outward.

The case of cylindrical symmetry is considerably more complex to analyze, and only approximate theories have been developed. If we restrict the discussion to large R/a_o, where a_o is the initial cylinder radius, we may obtain approximate numerical results.

At large R/a_o, the cylindrical symmetry should become unimportant

and the pressure approaches that for a sphere of the same volume as the cylinder;

$$(61) \qquad \frac{4}{3}\pi a_o'^3 = \pi a_o^2 L$$

Or, the equivalent sphere has a radius;

$$(62) \qquad a_o' = \left(\frac{3L}{4a_o}\right)^{1/3} a_o$$

If an exponential shock $p_m e^{-t/\theta}$ is assumed, it is found that the peak axial pressure should decay as $(a_o/R)^{.6}$ near the charge, to $(a_o/R)^{1.15}$ at distances greater than the charge length[24]. The transition should occur at $R \approx L/2$.

Accordingly, the peak pressure due to an underwater spark discharge at a distance $R >> L/2$, should be;

$$(63) \qquad p_m \approx p_o \left(a_o/L/2\right)^{.6} \left(\frac{L/2}{R}\right)^{1.15}$$

An approximate expression for the time constant θ at a distance $R >> L/2$ may be found by using the asymptotic expression for the time constant of a spherical shock wave;

$$(64) \qquad \theta \approx 4 \frac{a_o}{C_o^3} \frac{p_o}{\rho} \log_e\left(\frac{R}{a_o}\right)$$

In (64), ρ is the density corresponding to the pressure p_o which may be determined from the equation of state for water[25],

$$p_o = \frac{\rho_o C_o^2}{7}\left[\left(\frac{\rho}{\rho_o}\right)^7 - 1\right] \tag{65}$$

It is interesting to note that the asymptotic time constant θ does not depend directly upon the time constant of the external pressure at the plasma water boundary. In fact, as we will see, θ will in general be many times greater than τ.

It is evident that the peak pressure falloff in excess of acoustic and the time spread of the shock wave will result in a dependence of the energy flux upon distance. It is found for underwater explosions that the energy flux is not as dependent upon range as the peak pressure since it represents an integration of the entire pressure time curve and the effects of large peak pressures are smoothed out.

IV. THE ELECTRICAL PROPERTIES OF THE UNDERWATER SPARK DISCHARGE

1. An Approximate Equivalent Circuit

An approximate equivalent electrical circuit for the underwater spark discharge may be obtained. If the variations of plasma conductivity σ with time are neglected, the electrical resistance of the plasma is,

$$R_g \approx R_o/x^2 \tag{66}$$

where,

$$R_o = \frac{L}{\sigma a_o^2} \tag{67}$$

The variation of x with t is given by (23). If R_o is sufficiently large compared to the series loss resistance of the discharge circuit and the reactance of the series loss inductance, the equivalent circuit of figure 11 may be drawn.

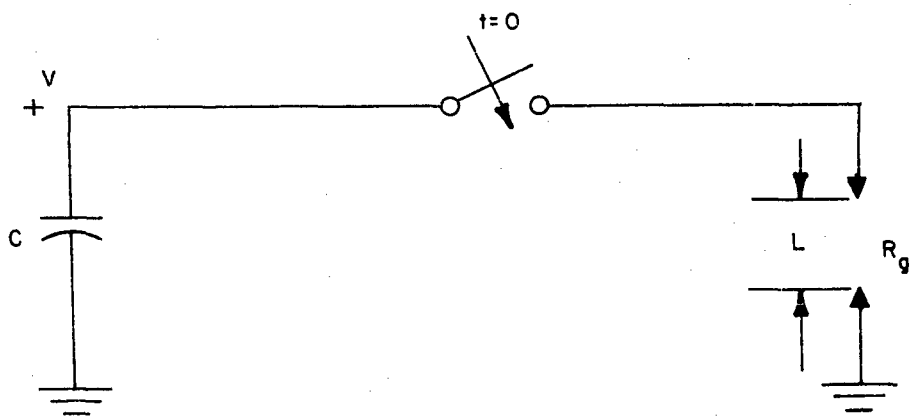

Figure 11. Underwater Spark Discharge Approximate Equivalent Circuit

The storage capacitance C is assumed to be charged to a potential V, and at t = 0, breakdown occurs. The following differential equation may be written;

$$R_g \frac{dq}{dt} + q/C = 0 \tag{68}$$

Where the initial condition, q (o) = CV must be satisfied. The variables are easily separated giving;

$$\frac{dq}{q} = -1/C \int_o^t \frac{dt}{R_g} \tag{69}$$

Transforming to the x variable from (21) and using (66);

$$\log q = -\frac{2\tau}{R_o C} \int_1^x \frac{x^4}{(x^2-1)^{1/2}}\, dx \tag{70}$$

After performing the integration , and using the initial condition, we obtain the following solutions;

$$V = V\exp\left\{-\frac{2\tau}{R_o C}\left[x^3 (x^2-1)^{1/2} - 3/4\, x\, (x^2-1)^{3/2} - 3/8\, x\, (x^2-1)^{1/2} + \frac{3}{8}\cosh^{-1} x\right]\right\} \tag{71}$$

and,

$$i = V/R_o\, x^2 \exp\left\{\frac{-2\tau}{R_o C}\left[x^3 (x^2-1)^{1/2} - \frac{3}{4}\, x\, (x^2-1)^{3/2} - 3/8\, x\, (x^2-1)^{1/2} + 3/8 \cosh^{-1} x\right]\right\} \tag{72}$$

Using (24), for $x > 1.2$, $t/\tau > 1.3$ these expressions become

$$v \approx V \exp\left[-\frac{\tau}{2R_oC} (t/\tau)^2\right] \tag{73}$$

and,

$$i \approx V/R_o \ (t/\tau) \exp\left[-\tau/2R_oC \ (t/\tau)^2\right] \tag{74}$$

Equations (73) and (74) may be used to solve for the instant of maximum current, the current at maximum, the voltage at the instant of maximum current, and the plasma resistance. The following relationships are obtained;

$$\begin{cases} t_m \approx \sqrt{R_oC\tau} & \text{(a)} \\ i_m \approx .6\ V \sqrt{\dfrac{C}{R_o\tau}} & \text{(b)} \\ V_m \approx .6\ V & \text{(c)} \\ R_m \approx \dfrac{R_o\tau}{C} & \text{(d)} \end{cases} \tag{75}$$

By referring to figure 3, it is evident that the form of (73) and (74) is matched to the experimental current and voltage waveforms.

2. Pinch Pressure

The magnetic field set up by the current flowing through the spark channel produces average forces on the charged particles tending to force them together. The net reduction of pressure on the constraining envelope produced by this effect is known as the pinch pressure.[26, 27]

If we assume the total current to be uniformly distributed over the cross-sectional area of the plasma, the pinch pressure is,

$$p_{pinch} = \frac{\mu_o \mu_r (a^2 - r^2) i^2}{4 \pi^2 a^4} \qquad r \leq a \tag{76}$$

where $\mu_o = 4\pi (10)^{-7}$ henry s/meter

This parabolic pressure distribution when integrated over the channel cross-section, gives an average pinch pressure of;

$$\bar{p}_{pinch} = \frac{\mu_o \mu_r i^2}{8 \pi^2 a^2} = \frac{i^2 (10)^{-7}}{2 \pi a^2} \quad \frac{\text{newtons}}{\text{meter}^2} \tag{77}$$

If $t/\tau > 1.3$, the approximations (25) and (74) may be used in (77) to obtain the pinch pressure as a function of time.

$$\bar{p}_{pinch} = \frac{V^2}{R_o^2 a_o^2} (t/\tau) \exp\left[- \tau / R_o C (t/\tau)^2 \right] \tag{78}$$

The maximum pinch pressure occurs at a time;

$$t_{m_{pinch}} = \sqrt{\frac{R_o C \tau}{2}} \text{ seconds} \tag{79}$$

The maximum value of the average pinch pressure is;

$$(80) \qquad \bar{p}_{pinch_{MAX.}} = \frac{.55\,(10)^{-7}\,V^2\,C^{1/2}}{R_o^{3/2}\,\tau^{1/2}\,a_o^2} \quad \frac{\text{newtons}}{\text{meter}^2}$$

It has been found that the magnitudes of the underwater spark discharge pinch pressures are sufficiently small so as to have a negligible effect upon the observable properties of the underwater spark discharge.

V. COMPARISON WITH EXPERIMENT

A comparison of the theoretical results with experimental data will be made for an underwater spark discharge having the parameters,

$$V = 30 \text{ kilovolts}, \quad C = .1\ \mu f, \quad L = 4 \text{ cm}, \quad E = 45 \text{ joules}.$$

These parameters were selected since Frolov and Roi[28] provide measured current, voltage and pressure waveforms for these values.

Current and Voltage Waveforms

When the parameter $R_o\tau$ in equations (75) is known, the theory predicts the expected current and voltage waveforms. However, $R_o\tau$ must be determined from one of the experimental values. Since the time between breakdown and current maximum appears to be insensitive to minor variations, the experimental value of $t_m = 1.1\ \mu sec$ will be used. Equation (75a) then allows us to calculate $R_o\tau = 12.1\ (10)^{-6}$. This value has been used in (73) and (74) to calculate the theoretical current and voltage waveforms which are plotted in figure 12 along with the experimental curves. The differences may be resolved qualitatively.

Martin[29] determines the variation of plasma conductivity during the discharge. The conductivity is found to increase to a maximum near the instant of maximum current and then decrease. If the plasma conductivity behaved in the same manner in this case, it would explain the fact that the experimental current becomes greater than the theoretical value near the current maximum, and then drops more rapidly than the theoretical curve.

In order to evaluate the theoretical results for the acoustic properties,

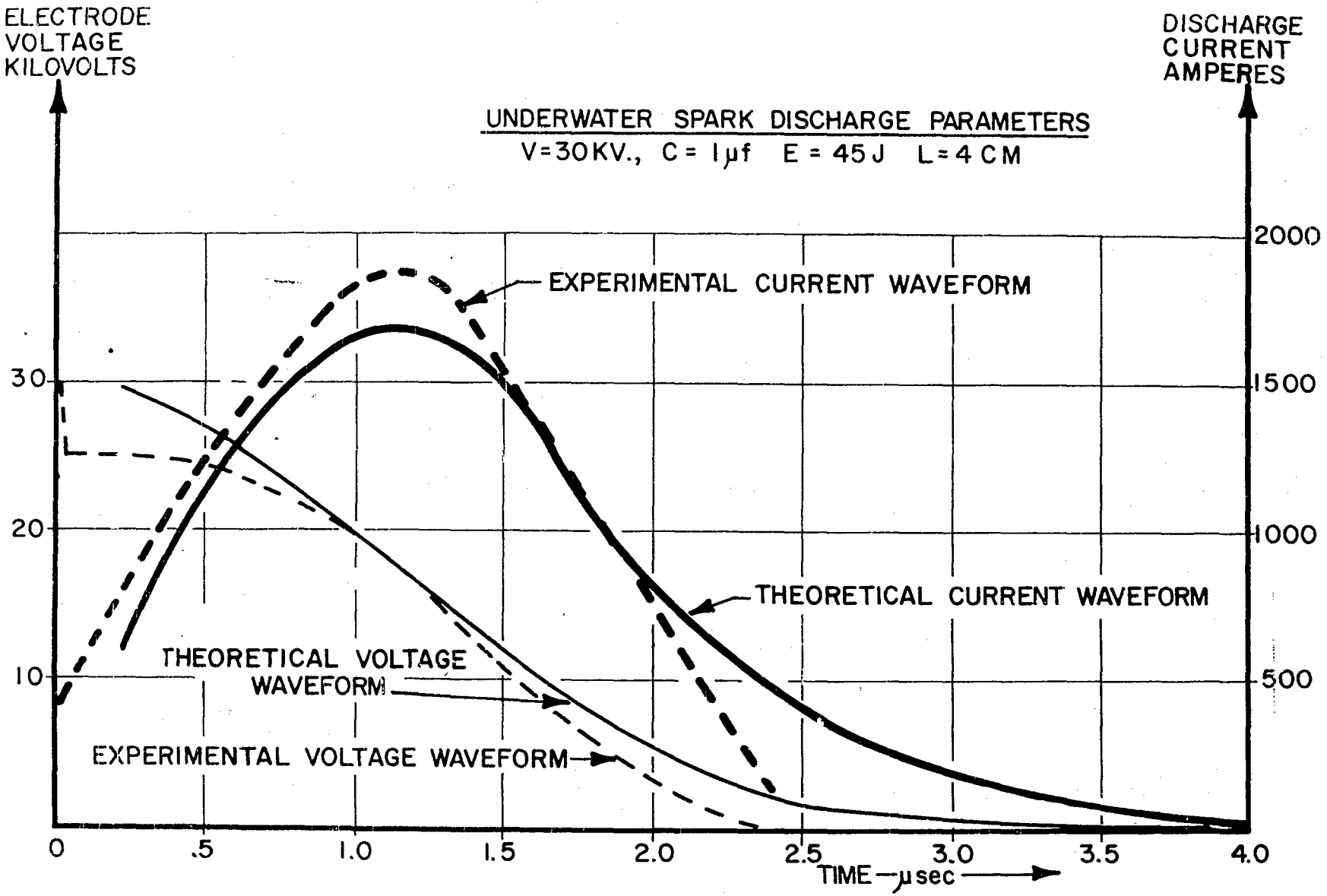

Figure 12 Theoretical and Experimental Current and Voltage Waveforms

a value of τ is necessary. An approximate estimate may be obtained from the experimental current and voltage values after breakdown, which are $V \approx 25$ kilovolts, $I \approx 370$ amperes. Dividing these values, we obtain a value of $R_o = 68$ ohms. Using the previously determined value of $R_o\tau = 12.1\,(10)^{-6}$, a value of $\tau = .18\,\mu$sec is obtained.

The approximate equations, (73) and (74), should be valid for $x > 1.2$, $t > 1.3$, or $t > .235\,\mu$sec, which covers the greater part of the current and voltage curves.

Acoustic Properties

A numerical evaluation of the theoretical results for the acoustic properties of the underwater spark discharge must be based upon estimated values of τ and Y. Since the electrode voltage drops at the instant of breakdown from 30 kilovolts to about 20 kilovolts at current maximum approximately a microsecond later, it appears reasonable to pick the energy represented, 25 joules, as a value of Y. This value of Y, together with the estimated value of τ permit (24) and (26) to be solved simultaneously for p_o and a_o. The calculated values are,

$p_o = 12,200$ atmospheres

$a_o = .4$ mm

These values may be used to check the assumption of incompressibility which is valid provided the wall velocity is much less than the speed of sound. The calculated maximum wall velocity is from (34);

$$da/dt_{MAX} = \frac{a_o}{4\tau} = \frac{(.4)\,(10)^{-3}}{(4)(.18)(10)^{-6}} = 555 \text{ meters/sec}$$

The velocity of sound is 1500 meters/sec, so that the maximum wall velocity is about 1/3 that of sound. If it is remembered that this maximum velocity exists over a short part of the expansion of the plasma, the assumption of incompressibility appears reasonable.

The external pressure at the plasma wall calculated from (39) is shown in figure 13. The fact that the time scale is much less than that of the current and voltage waveforms is evident.

The peak pressure which should be measured at a distance R from the plasma, in a direction normal to the channel may be calculated by means of the shock wave relationships. Using (63);

$$p_m \approx p_o \left(a_o/L/2 \right) \cdot 6 \left(\frac{L/2}{R} \right)^{1.15} = \left(\frac{4\,(10)^{-4}}{2\,(10)^{-2}} \right) \cdot 6 \left(\frac{2(10)^{-2}}{1} \right)^{1.15} \quad (12,500)$$

$$p_m \approx 1.1\,(10)^{-3} \quad (12,500) = 13.8 \text{ atmospheres}$$

Experimentally, a peak pressure of 9 atmospheres is measured at that distance by a piezoelectric probe with a frequency response specified as uniform up to 800 kc. The difference between the calculated and experimental values may be due in part to the frequency response of the probe.

The approximate value of the time constant at this distance may be calculated from (64);

$$\theta \approx \frac{4a_o}{C_o^3} \frac{p_o}{\rho} \log_e (R/a_o = \frac{(4)(4)(10)^{-4}\ 12.2\,(10^8}{(1.5)^3\ (10)^9} \log_e \frac{1}{4(10)^{-4}}$$

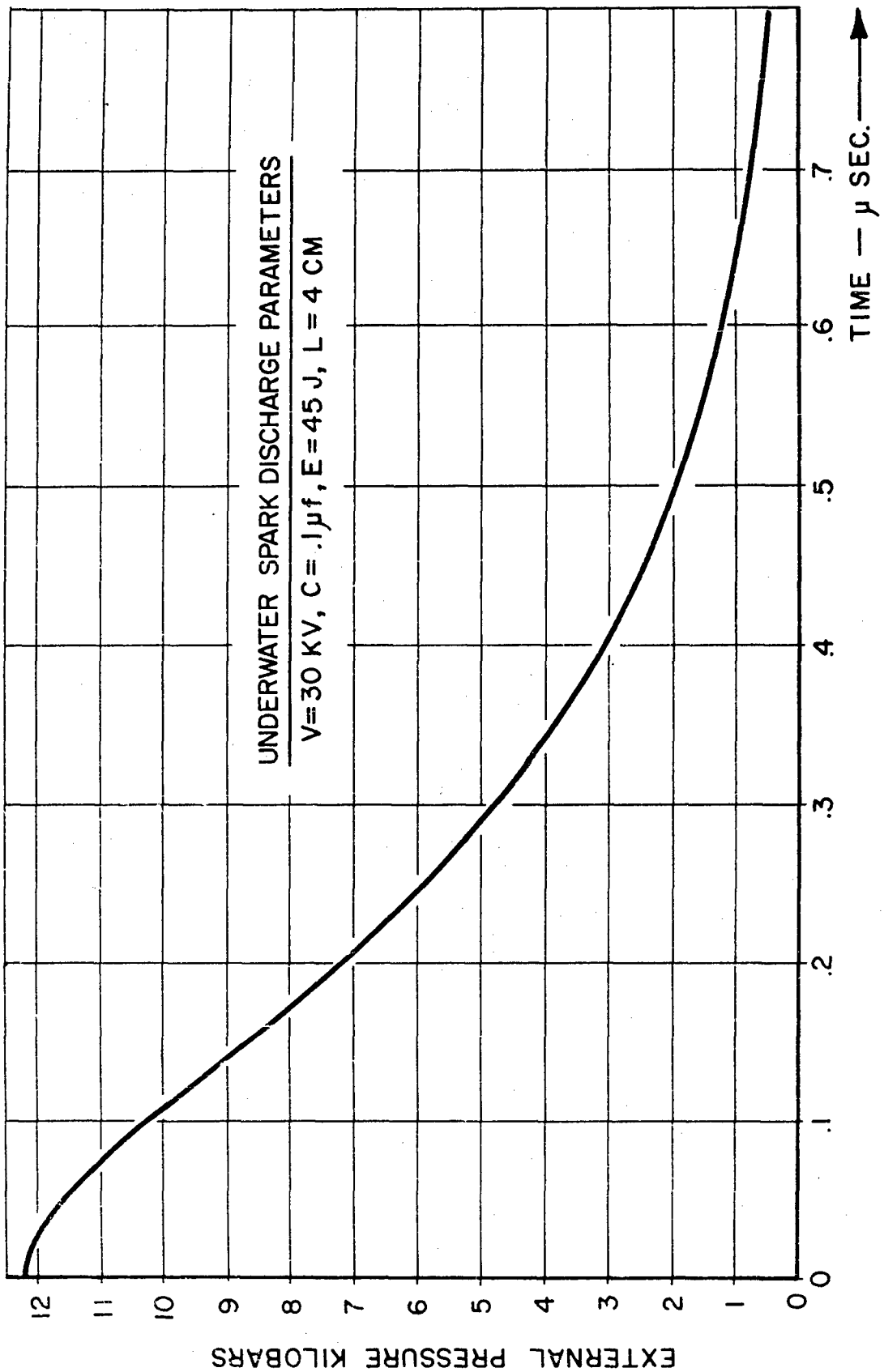

Figure 13 Calculated External Pressure Vs. Time

$\theta \approx 4.45\ \mu sec$

The measured value is approximately 5 μsec.

Since the time constant at the plasma-water boundary was calculated as .36 μsec, the time scale appears to have increased by about a factor of 12.

Using the theory for the directional properties of the pressure waveform, the amplitude and duration of the waveform in a direction parallel to the spark channel may be calculated. In this direction,

$$\Delta\tau = L/c \sin\theta = \frac{4\,(10)^{-2}}{1.5\,(10)^{3}} = 27.6\ \mu sec$$

The calculated time constant at 0° may be used to obtain $\propto L/c$,

$$\propto L/c = \frac{4\,(10)^{-2}}{4.45\,(10)^{-6}\ 1.5\,(10)^{3}} = 5.9$$

We may obtain the peak pressure at 90° from (49);

$$P_{Rpeak} = \frac{p_o\left[1 - e^{-\propto L/c}\right]}{\propto L/c} = \frac{13.8}{5.9} = 2.34 \text{ atmospheres.}$$

A value of 2 atmospheres is measured experimentally.

The experimental and theoretical waveforms for directions normal and parallel to the underwater spark discharge plasma are shown in figure 14.

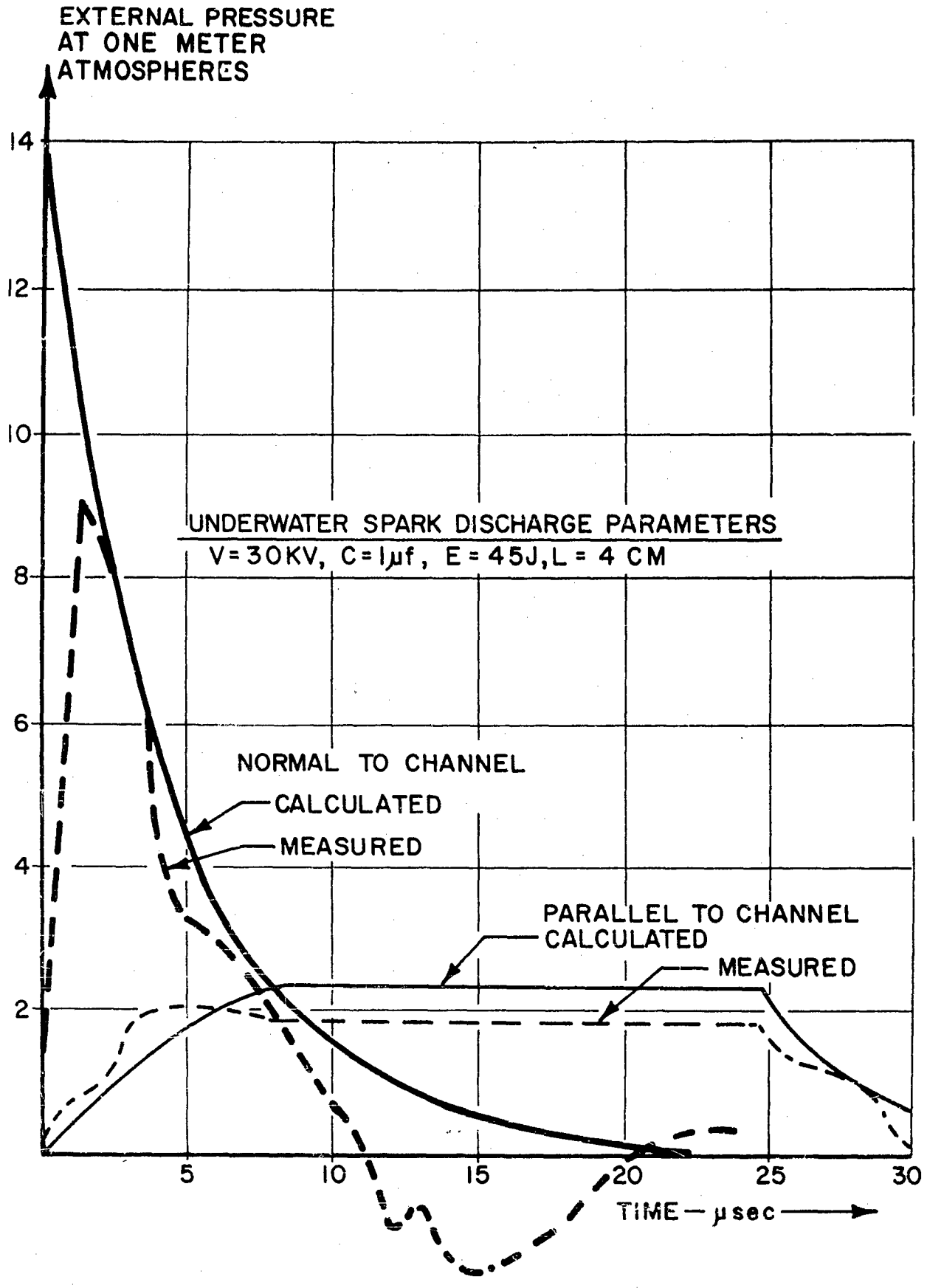

Figure 14 Theoretical and Experimental Pressure-Time Curves

The agreement between the calculated and measured values is better in the parallel direction since the probe is not required to pass a steep-fronted pressure waveform, as it is in the normal direction.

Pinch Pressure

The maximum average pinch pressure may be calculated from (80);

$$p_{pinch_{MAX}} = \frac{(.55)(10)^{-7}\, V^2\, C^{1/2}}{R_o^{3/2}\, \tau^{1/2} a^2_o} = \frac{(.55)\,(10)^{-7}(9)(10)^{8}(10)^{1/2}(10)^{-4}}{(68)^{3/2}(18)^{1/2}(10)^{-4}(16)(10)^{-8}}$$

$$= 4.1\,(10)^{5}\ \frac{\text{newtons}}{m^2}$$

The calculated pinch pressure of 4.1 atmospheres is sufficiently small so that the error introduced by neglecting the effects of the pinch pressure upon the equation of motion are negligible.

Martin calculated the pinch pressure[29] for an underwater spark discharge having the parameters, V = 25 kilovolts, C = 5.8 μf, L = 1.5 cm. He found the maximum average pinch pressure to be 735 atmospheres for a peak current of 85,000 amperes. It may be concluded that the contribution of the pinch pressure to the kinetic pressure of an underwater spark discharge is not significant.

Electro-Acoustic Efficiency

The experimental energy flux directivity factor may be obtained by calculating the energy flux radiated in a direction normal to the discharge, and relating it to the total energy radiated.

If the waveform measured normal to the discharge plasma were the same over a sphere of radius R;

$$E_{Normal} = \frac{4\pi R^2 p^2_R}{2\rho_o c} = \frac{(4\pi)(81)(10)^{10}(5)(10)^{-6}}{(2)(10)^3(1.5)(10)^3} = 17 \text{ joules}$$

Frolov and Roi[2] report an electro-acoustic efficiency of 32% which they calculate by integrating pressure-time curves measured over a spherical segment of 1 meter radius. On the basis of the definition of the energy flux directivity factor η_D from (58);

$$\eta_D = \int_0^{2\pi}\int_0^{\pi} \frac{\phi(\theta)}{\phi_{Normal}} \sin\theta \, d\theta \, d\psi = \frac{(.32)(45)}{17} = .85$$

Using the value of η_D calculated above, (60) may be used to calculate the acoustic efficiency;

$$\eta_A \approx \frac{\eta_D}{c}\sqrt{\frac{p_o}{\rho}} = \frac{.85}{1.5(10)^3}\sqrt{\frac{12.2(10)^8}{(10)^3}} = .62$$

Therefore, the total electro-acoustic efficiency should be;

$$\eta_T = \frac{Y}{E} \cdot \eta_A = \frac{25}{45}(.62) = 34.4\%$$

The measured efficiency should be lower since in the derivation of (60) shock wave energy losses were neglected.

The good agreement between the calculated and measured acoustic

parameters appears to justify the value of Y = 25 joules, which was selected as the energy available for the motion of the spark discharge plasma.

VI. SUMMARY

A theoretical investigation of the electro-acoustic properties of the underwater spark discharge has been presented. Equations for the conservation of the mass and momentum of an incompressible fluid have been used to derive approximate expressions for the kinetic and potential energies of flow outside the plasma-water boundary. Setting the sum of these energies equal to a constant resulted in an equation of motion involving the plasma radius, wall velocity, and external pressure.

Assuming adiabatic expansion of the plasma, a relationship between the external pressure and plasma volume was obtained. This relationship permitted an explicit solution of the equation of motion for the plasma radius as a function of time. The solution obtained was expressed in terms of the ratio of the plasma radius, a, to its initial radius, a_o, and the ratio of the time, t, to a characteristic time, τ, which was found to be a function of the initial values of plasma radius, and external pressure. For $a/a_o >> 1$ the calculated radius becomes almost directly proportional to the square root of the time, a result which is in agreement with experimental observations.

The calculated plasma radius as a function of time and the adiabatic pressure-volume relationship enabled the external pressure at the plasma wall to be determined. The external pressure was found to be approximately an exponential function of time with a time constant of 2

An exponential approximation for the external wall pressure was used in the derivation of the directional distribution of the radiated pressure pulse. From the agreement between the experimental and calculated

pressure-time curves in directions normal to and parallel to the spark channel axis, one may conclude that to a good approximation the underwater spark discharge behaves as a uniform linear acoustic source radiating an exponential waveform.

Finite amplitude effects have been discussed through application of the shock wave propagation theory developed for an underwater explosion. Major effects such as peak pressure falloff in excess of acoustic and broadening of the waveform as it propagates outward have been discussed.

By neglecting the variation of the plasma conductivity with time, and utilizing the equation of motion for variation of the spark channel area, an expression for the plasma resistance has been derived. This resistance, together with a simple electrical equivalent circuit has been used to obtain theoretical discharge current and voltage waveforms.

These results show that measurable quantities associated with the experimental current and voltage waveforms may be used to estimate parameters, such as the initial energy available for plasma motion, Y, and the characteristic time τ. Once they are known, these quantities allow the prediction of other electro-acoustic properties of an underwater spark discharge. Quantities such as initial peak wall pressure and channel radius, which are not easily obtainable by experimental methods, may be calculated by utilizing a set of simultaneous equations.

Through the above techniques, the initial wall pressure and plasma radius for a 30 kv, .1 μfd, 45 joule underwater spark discharge have been calculated. The values obtained for p_o and a_o were respectively, 12, 200 atmospheres, and .4 mm. Using these values, the properties of the

radiated pressure pulse have been determined and found to be in good agreement with the experimental results.

VII. PRACTICAL APPLICATIONS

A number of areas exist in which the underwater spark discharge may be of great practical utility.

At the present time, several large organizations are investigating the application of the underwater spark discharge to metal forming. A number of difficult forming jobs have been performed quite rapidly by placing the piece to be formed between a die and an underwater spark discharge.[30]

Another application for the underwater spark discharge is a sonic source for underwater echo sounding. Specific applications are classified information and cannot be mentioned; however, the underwater spark discharge shows great promise in this area.[31]

The underwater spark discharge might be used for an investigation of the elastic constants of materials under high transient stress. Through measurements of refracted and unrefracted shock fronts at a water-metal boundary, the velocity of the shock wave in the material could be calculated, and the elasticity of the material obtained.[32, 33]

VIII. SUGGESTIONS FOR FUTURE STUDY

There is a great amount of work which remains to be done before the underwater spark discharge will be as well understood as some of the other types of gaseous discharges.

A detailed analysis of the breakdown of a water gap and the initial stages of plasma formation, from both a theoretical and experimental point of view, would be valuable. Such a study might be similar to the one performed by Martin[1], except that a number of different parameter combinations would be employed. This investigation should include a detailed determination of the electrical characteristics of discharges occuring in water of controlled temperature and salinity. In particular, the variation of plasma conductivity with time should be measured. This study would be similar to the one performed by Martin, except that a number of different parameter combinations might be employed.

In addition, an experimental investigation of the pressures which exist in the vicinity of the underwater spark discharge channel would be of interest. However, the problems connected with such measurements are formidable. If a pressure sensitive device were used, it would have to be small enough not to disturb the field; have a bandwidth of the order of several megacycles; be insensitive to stray pickup from extremely strong electromagnetic fields; and, finally, have sufficient strength to withstand the tremendous pressures involved. Needless to say, such a device may be hard to come by. Other techniques might be useful. For example, a measurement of the curvature of a light ray passing through a high pressure region would be an indication of the pressures involved.

The accuracy of such a measurement is limited by a knowledge of the variation of the refractive index of water with pressure and suitably accurate measurements may not be available.[34]

A related investigation might consist of a determination of electroacoustic efficiency as a function of voltage, energy, and gap separation. This study would be particularly valuable for voltages greater than 30 kilovolts and gaps longer than 5 cm, since Frolov and Roi[2] stopped their investigation at these values.

IX. BIBLIOGRAPHY

1. E. A. Martin, "The Underwater Spark: An Example of Gaseous Conduction at About 10,000 Atmospheres," University of Michigan, Engineering Research Institute, Report 2048-12-f, July 1956.

2. N. A. Roi and D. P. Frolov, "The Electro-Acoustic Efficiency of a Spark Discharge in Water," Doklady Akademii Nauk, 118 (1958) 4, p. p. 683-686.

3. R. H. Cole, "Underwater Explosions," Princeton University Press, New Jersey, 1948.

4. H. F. Willis, "Underwater Explosions, Time Interval Between Successive Explosions," British Report WA-47-21, 1941.

5. S. Gardner, "Acoustic Properties of Underwater Spark Discharges," U.S. Navy Journal of Underwater Acoustics, Vol. 10, No. 1, January 1960 (Conf.)

6. L. B. Loeb, "Basic Processes of Gaseous Electronics," University of California Press, Los Angeles, 1960.

7. R. Courant and K. Friedrichs, "Supersonic Flow and Shock Waves," Interscience Publishers, New York, 1948.

8. S. R. Brinkley Jr. and J. G. Kirkwood, "Theory of the Propagation of Shock Waves," Phys.Rev. 71, 606, 1947.

9. S. R. Brinkley Jr. and J. G. Kirkwood, "Theory of the Propagation of Shock Waves From Infinite Cylinders of Explosive", Phys. Rev., 72, 1109, 1947.

10. M. Ewing and A. Cray, "Multiple Impulses From Underwater Explosions," Woods Hole Oceanographic Inst. 1941.

11. C. Herring, "Theory of the Pulsations of The Gas Bubble Produced By an Underwater Explosion," NDRC Division 6, Report C4-Sr 20, 1941.

12. L. Kinsler and A. Frey, "Fundamentals of Acoustics," John Wiley and Sons, New York, 1950.

13. H. Lamb, "Hydrodynamics," 6th Edition, Cambridge University Press, 1932.

14. M. Zemansky, "Heat and Thermodynamics," McGraw Hill Book Company, New York, 1943.

15. Martin, loc. cit. P. 152.

16. L. Spitzer, Jr., "Physics of Fully Ionized Gases", Interscience Publishers Inc., New York, 1956.

17. Martin, loc. cit., P. 117.

18. B. Friedman, "Theory of Underwater Explosion Bubbles", Report IMM - N. Y. U. 166, Institute for Mathematics and Mechanics, New York University.

19. A. B. Arons and D. R. Yennie, "Energy Partition in Underwater Explosion Phenomena", Rev. Mod. Phys., 20, 519, 1948.

20. A. B. Arons and D. R. Yennie, "Long Range Shock Propagation in Underwater Explosion Phenomena". NavOrd Report No. 424, April 1949.

21. J. G. Kirkwood and S. R. Brinkley Jr., "Theory of the Propagation of Shock Waves From Explosive Sources in Air and Water", OSRD 4814, 1945.

22. M. F. M. Osborne and A. H. Taylor, "Non-linear Propagation of Underwater Shock Waves", Phys. Rev., 70, 322, 1946.

23. Cole, loc. cit. p. 110.

24. Cole, loc. cit. p. 126.

25. Courant, loc. cit. p. 8.

26. L. C. Burkhardt, "Pinch Effect", Journ. Appl. Physics, Vol. 28, No. 5, May, 1957.

27. Martin, loc. cit. p. 118.

28. Frolov and Roi, loc. cit. p. 4.

29. Martin, loc. cit. p. 154.

30. "Explosive Forming", Electronic Industries, May 1961, p. 100.

31. H. H. Rust and H. Drubba, "Praktishe Anwendung des Unterwasser Funkens als Impuls-Schallgeber fur die Echolotung", Zeitschrift fur Angewandte Physik, 5, 251 (1953)

32. J. M. Walsh and R. H. Christian, "Equation of State of Metals From Shock Wave Measurements", Physical Review, 97, 1544, 1955.

33. J. S. Rinehart and J. Pearson, "Behavior of Metals Under Impulsive Loads", American Society for Metals, Cleveland, 1954.

34. P. W. Bridgman, "The Physics of High Pressures", Bell and Sons, London, 1949.

X. APPENDIX I

$$(A-1) \qquad p_R(t, \Delta\tau) = \int_{-\Delta\tau/2}^{+\Delta\tau/2} e^{-\alpha(t-z)}\, U(t-z)\, dz$$

Making the substitution $v = t - z$,

$$(A-2) \qquad p_R(t, \Delta\tau) = 1/\Delta\tau \int_{t-\Delta\tau/2}^{t+\Delta\tau/2} e^{-\alpha v}\, U(v)\, dv$$

Recognizing that since the step occurs only when its argument equals zero, the value of the integral depends upon restrictions placed upon its limits,

$$(A-3) \qquad p_R(t, \Delta\tau) = \begin{cases} \dfrac{1}{\Delta\tau} \displaystyle\int_{t-\Delta\tau/2}^{t+\Delta\tau/2} e^{-\alpha v}\, dv & t \geq \Delta\tau/2 \\ \dfrac{1}{\Delta\tau} \displaystyle\int_{0}^{t+\Delta\tau/2} e^{-\alpha v}\, dv & t \leq \Delta\tau/2 \end{cases}$$

The solution becomes;

(A - 4)

$$p_R(t, \Delta\tau) = \begin{cases} \dfrac{\sinh(\alpha\Delta\tau/2)}{\alpha\Delta\tau/2}\, e^{-\alpha t} & t \geq \Delta\tau/2 \\ = \dfrac{1}{\alpha\Delta\tau}\left[1 - e^{-\alpha t}\, e^{-\alpha\Delta\tau/2}\right] & -\Delta\tau/2 \leq t \leq \Delta\tau/2 \\ = 0 & t \leq -\Delta\tau/2 \end{cases}$$

DISTRIBUTION LIST FOR EDO CORPORATION SPARK SOURCE REPORT

Contract No. NOnr2288(00)

Office of Naval Research (Code 411)
Department of the Navy
Washington 25, D. C. (5 copies)

Director
U. S. Naval Research Laboratory
Technical Information Division
Washington 25, D. C. (6 copies)

Director
U. S. Naval Research Laboratory
Sound Division
Washington 25, D. C. (1 copy)

Commanding Officer
Office of Naval Research Branch Off.
Box 39, Navy No. 100
FPO, New York (10 Copies)

Office of Technical Services
Department of Commerce
Washington, D. C. (1 copy)

Armed Services Tech. Information Agcy.
Arlington Hall Station
Arlington 12, Virginia (10 copies)

Commander
U. S. Naval Ordnance Laboratory
Acoustics Division
White Oak
Silver Spring, Md. (1 copy)

Commanding Officer and Director
U. S. Navy Electronics Laboratory
San Diego 52, Calif. (1 copy)

Director
U. S. Navy Underwater Sound Ref. Lab.
Office of Naval Research
P. O. Box 8337
Orlando, Florida (1 copy)

Commanding Officer and Director
U. S. Navy Underwater Sound Lab.
Fort Trumbull
New London, Conn. (1 copy)

Commander
U. S. Naval Air Development Center
Johnsville, Penna. (1 copy)

Commanding Officer and Directc
David Taylor Model Basin
Washington 7, D. C. (1 copy)

Director
National Bureau of Standards
Connecticut Ave. & VanNess St.
Washington 25, D.C. (1 copy)
(Attn: Chief of Sound Section)

Office of Chief Signal Officer
Department of the Army
Pentagon Building
Washington 25, D. C. (1 copy)

Superintendent
U. S. Navy Postgraduate School
Monterey, Calif. (1 copy)
(Attn: Prof. L. E. Kinsler)

Commanding Officer
Air Force Cambridge Research (
230 Albany Street
Cambridge 39, Mass. (1 copy)

Commanding Officer
U. S. Navy Mine Defense Lab.
Panama City, Florida (1 copy)

U. S. Naval Academy
Annapolis, Md.
(Attn: Library) (1 copy)

Harvard University
Acoustics Laboratory
Division of Applied Science
Cambridge 38, Mass. (1 copy)

University of California
Marine Physical Laboratory of
Scripps Institution of
Oceanography
San Diego 52, Calif. (1 copy)

Director
Columbia University
Hudson Labs
145 Palisade Street
Dobbs Ferry, N. Y. (1 copy)

Woods Hole Oceanographic Institution
Woods Hole, Mass. (1 copy)

U. S. Navy SOFAR Station
APO #856, c/o Postmaster
New York, N. Y.
Attn: Mr. G. R. Hamilton (1 copy)

Defense Research Laboratory
University of Texas
Austin, Texas (1 copy)

Chief, Bureau of Ships
Code 689B
Department of the Navy
Washington 25, D. C. (1 copy)

Ordnance Research Laboratory
Pennsylvania State University
University Park, Penna. (1 copy)

Commander
U. S. Naval Ordnance Test Station
Pasadena Annex
3202 E. Foothill Blvd
Pasadena 8, Calif. (1 copy)

Chief, Bureau of Naval Weapons
Code RUDC-5
Department of the Navy
Washington 25, D. C. (1 copy)

Chief, Bureau of Ships
Code 450X (Mr. Earl Palmer)
Department of the Navy
Washington 25, D. C. (1 copy)

Mr. William L. Cloninger
Librascope Division
General Precision, Inc.
1234 Airway
Glendale, Calif. (1 copy)

Dr. G. S. Bennett
Chrysler Corporation Missile Division
P. O. Box 2628
Detroit 31, Michigan (1 copy)

Mr. Robert J. Urick
Acoustics Division
U. S. Naval Ordnance La
White Oak
Silver Spring, Md. (1 c

Dr. W. A. Huggins
Johns Hopkins Universit
Department of Electrica
Baltimore 18, Md. (1 co

Bureau of Naval Weapons
c/o Ford Instrument Co
31-10 Thomson Ave.
Long Island City, N. Y.
(Information copy)